KINETIC BEHAVIOR OF COUPLED REACTOR CORES

by

Richard Arlen Danofsky

A Thesis Submitted to the
Graduate Faculty in Partial Fulfillment of
The Requirements for the Degree of
MASTER OF SCIENCE

Major Subject: Nuclear Engineering

Iowa State University
Of Science and Technology
Ames, Iowa

1960

TABLE OF CONTENTS

INTRODUCTION

The determination of the time behavior of the reactor system is an important part of any nuclear reactor design study. Information on how the reactor responds to step, ramp and sinusoidal inputs of reactivity is useful to the control system designer and in the formulation of the hazards report of the proposed system.

These responses are usually determined by solving the time dependent neutron diffusion equation which is derived by assuming that the reactor can be treated as a black box having an average neutron density, a neutron lifetime, and a reactivity $\frac{\delta K}{K}$. A system of seven differential equations must be solved, one equation for the neutron flux and six equations for the delayed neutron precursors. A reactor simulator or an analog computer is a convenient device for solving these differential equations for various values of the reactor parameters which effect the time behavior of the system. It is usually assumed that the spatial variation of the neutron flux in the reactor core does not effect the kinetic response of the system. As pointed out by Schultz (29, p. 29), the one-point black box treatment yields kinetic answers, which for most systems, are consistent with experimental accuracy.

For some reactors however, the assumption that the flux distribution in the core does not effect the time behavior

of the reactor is not valid. Reactor cores which consist of distinct multiplying or fuel bearing regions separated by a moderating material give rise to the case in which the effect of the shape of the neutron flux distribution on the time behavior of the system must be considered. This means that the position and time variables are inseparable. The degree of inseparability would depend upon the spacing distances between multiplying regions and also upon the type of moderating material placed between the regions. As pointed out by Henry and Curlee (16) the degree of nonseparability depends on the neutron cross sections and diffusion coefficients throughout the reactor and especially on the thickness of the moderating region. Large separation distances correspond to large degrees of nonseparability of the variables.

Several existing reactor systems have cores similar to that described in the previous paragraph (2, 23). The UTR-10 reactor has a core which consists of two separate fuel bearing regions separated by approximately 46 centimeters of graphite. The migration length of neutrons in graphite is approximately 54 centimeters, and consequently it was assumed that this system would be one in which the spatial and time variations of neutron flux could not be assumed to be separable.

The purpose of this investigation was to study the kinetic response of the UTR-10 reactor to various input

disturbances of reactivity. The reactor kinetic equations were derived assuming that space and time variations of neutron flux are inseparable. These equations were then solved, with the aid of an analog computer, for step, ramp, and sinusoidal variations of reactivity.

The UTR-10 was chosen for this study for several reasons. It was planned that the results of this investigation could be used as an aid in planning future experiments with the UTR-10 reactor at Iowa State University. Also, values for constants which appear in the reactor kinetic equations were available for this system. It was hoped that this work would also provide information on the effects of the inseparability of space and time variation of neutron flux on control rod calibration. The effects of a reactivity oscillator placed in the central stringer in the graphite between core tanks was also studied.

LITERATURE SURVEY

Since the primary objective of this investigation was to study the kinetic behavior of a reactor for various types of reactivity disturbances using an analog computer, the purpose of the literature search was to review work performed by other investigators on reactor kinetics problem similar to that considered here. Coincidental with this, there was also an interest in the use of analog computers for solving the time dependent reactor equations and uses of computers as reactor simulators.

General Kinetics Equations

The development of the reactor kinetic equations normally used in time behavior studies is presented in (9, 10, 13, 17, 19, and 24). In all of these references the reactor kinetic equations are derived assuming that space and time variables are separable. The resultant equations consist of one first order differential equation which describes the variation of neutron density or flux with time, and six first order equations which describe the time variations of the six delayed neutron precursor concentrations. These equations may have constant coefficients (for a step input of reactivity) or the constants may be functions of time (ramp or sinusoidal input).

In most of the examples considered in these references

it was assumed that the six delayed neutron groups could be combined into one group having the weighted properties of the six groups. Keepin and Wimett (21) present the latest delayed neutron data for most of the fissionable nuclides.

Nonseparable Space and Time Variations of Neutron Flux

Henry and Curlee (16) presented a method for calculating the detailed kinetic response of a reactor during a transient when the space and time variables are not separable. A reactor model consisting of two slab regions containing coolant water and uranium bearing fuel plates and separated by a pure moderator was used to illustrate the method. The variation of the neutron level with time in each region following a 40°F drop in the inlet temperature to one of the slabs was considered. It was shown that semi-independent time behavior was possible with different variations in relative neutron level in each slab.

Baldwin (4) investigated the kinetics of the two core configuration of the Argonaut reactor. In this reactor two subcritical slabs two feet apart are immersed in a large graphite reflector. The system achieves criticality by the small interaction exchange of neutrons between the slabs. The kinetic equations were derived by writing a separate diffusion equation for each region and including a coupling interaction term for each region. The analysis accounted for

the fact that the ratio of fluxes in the two slabs can differ from unity but the stable reactor period is the same for both slabs. Foil activations have shown that the ratio of flux levels in the two slabs varies from unity to two due to flux tilting across the core regions.

The relationship between the stable reactor period and flux level ratios for various excess reactivities of each region was presented. The effect of flux tilting on rod calibration was discussed, and it was shown that the control rod worth as determined using inhour equation can be in error for the two slab system. The transfer functions for a two core reactor system were also derived.

Reactor Transfer Function

As pointed out in most texts on the stability of dynamic systems (8 and 28 for example), a knowledge of the steady state response of a system to a sinusoidal input can be used to study the characteristics of the transient response of the system. The phase and amplitude relationships between input and output variables as a function of frequency are described by the transfer function for the system with $j\omega$ substituted for the Laplace operator.

Harrer et al. (15) have shown experimentally that the concept of a transfer function for a reactor is valid. The theoretical and experimental frequency responses of the CP-2

reactor has been compared and good agreement was reported.

The expression for the transfer function for a single core reactor has been derived by Franz (11). The transfer function for a reactor relates the output (neutron density or flux) to input (reactivity). The reactor transfer function can be obtained by oscillating a control rod in a sinusoidal fashion or by using a reactivity oscillator. Griffin and Lundholm (14) described the use of reactor oscillators in the SRE and KEWB reactors. Baldwin et al. (5) discussed an oscillator used for measuring the transfer function of the Argonaut reactor.

Akcasu (1) has discussed a method of solving the reactor kinetic equations for sinusoidal variations in reactivity for large power excusions.

Analog Computers

The use of analog computers to study time behaviors of dynamic systems has found wide use in time dependent reactor studies (3, 6, 18, 20 and 25). A general discussion of analog computers is given by Korn and Korn (22). Reactor simulators are discussed by Schultz (29). Pagels (27) described a portable electronic reactor simulator and O'Meara (26) discussed reactor simulators. Braffort (7) discussed results obtained from an analog computer study of a reactor.

Franz and Alliston (12) described a reactor simulator

consisting of an analog computer which was used to train reactor operators for the PWR reactor. With this system it was possible to simulate the following:

1. Manual reactor startup.
2. Automatic and manual control rod adjustment.
3. Xenon transients.
4. Other operations associated with the power plant.

Many more references on the use of analog computers in reactor studies could be included, but it is felt that those listed above serve to indicate the importance of these devices in the field of Nuclear Engineering.

DEVELOPMENT OF THE MODIFIED REACTOR KINETIC EQUATIONS

The reactor kinetic equations for the UTR-10 reactor are derived in this section. The core of the UTR-10 consists of two multiplying regions which are cooled and moderated by water and separated by approximately 46 centimeters of graphite. Since this spacing is of the order of the migration length for neutrons in graphite it was assumed that there exists the possibility for semi-independent behavior of each region. By semi-independent behavior is meant that the average neutron flux level in one region can be different than the average neutron flux level in the other region during equilibrium or transient conditions. The flux distribution across the overall core can be tilted as illustrated in Figure 1. Since the kinetic response of the overall reactor system to various types of reactivity inputs depends upon how this flux is tilted, the time variation of the neutron level depends upon the spatial distribution of the neutron flux across the core. Therefore, if kinetic equations which are derived by assuming that the spatial distribution of the neutron flux does not effect the time behavior of the system are used, the results may be erroneous.

For purposes of analysis it was assumed that the two separate fuel regions of the reactor core could be treated as individual reactor cores with reactivity coupling between cores. Each region would be subcritical if it existed alone,

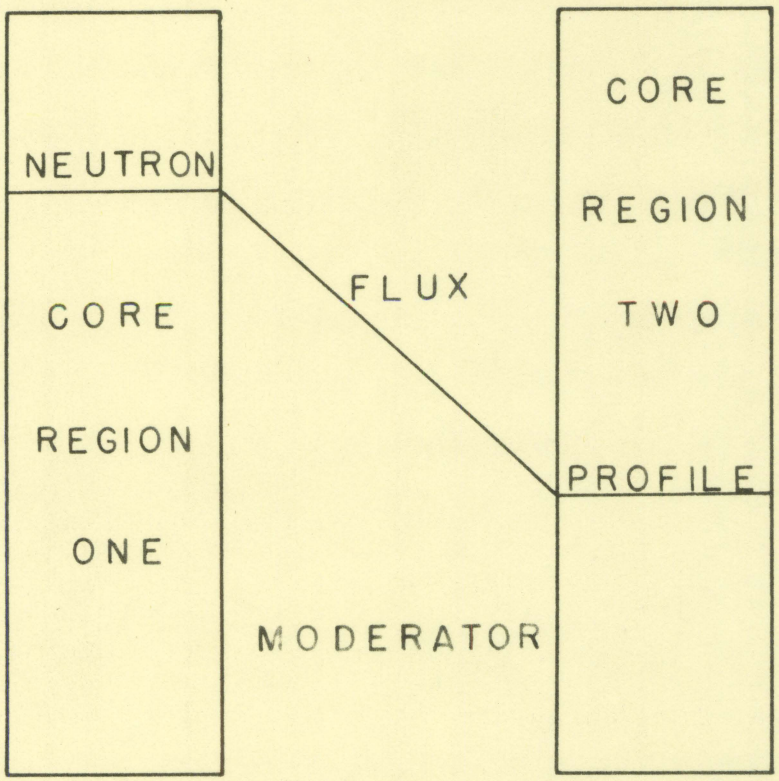

Figure 1. Flux tilting across the reactor core

but the coupling effect of the other region allows the system of two slabs to be critical or supercritical. Each core region was treated as a black box having an individual reactivity and average neutron density. It was assumed that the spatial distribution of neutron flux within a slab did not effect the behavior of that region. The reactivity coupling effect is due to the interaction exchange of neutrons between the two regions and it was assumed that the coupling effect of region 2 on region 1 is proportional to the average neutron flux in region 2 and the effect of region 1 on 2 is proportional to the average flux in region 1. This means that the shape of the neutron flux distribution across the two regions would effect the time behavior of the reactor.

It was assumed that a time dependent neutron level equation of the form

$$\frac{dn}{dt} = \delta K \frac{n}{\ell} - \beta \frac{n}{\ell} + \sum_{i=1}^{6} \lambda_i c_i + f(n) \qquad (1)$$

where

n = average neutron density in a fuel region, neutrons/cm^3

$\delta K = K_{eff} - 1$

ℓ = neutron lifetime in a finite medium, sec

β = total delayed neutron fraction

λ_i = decay constant for ith group of delayed neutron precursors, sec^{-1}

c_i = concentration of ith group of delayed neutron precursors, precursors/cm^3

f(n) = coupling effect, function of other core region could be applied to each of the fuel regions of the reactor core. A differential equation of this form, with the exception of the coupling term, is normally used to describe the kinetic behavior of a single region reactor (9, 19, 29). The differential equation for the delayed neutron precursor concentration in each slab was assumed to be

$$\frac{dc_i}{dt} = \frac{\beta_i n}{\ell} - \lambda_i c_i \,. \qquad (2)$$

As mentioned previously the reactivity coupling effect on one slab was assumed to be proportional to the average neutron flux in the opposite slab. Since some delay time is required before a change in neutron density in one core is reflected in the behavior of the opposite region, the coupling effect was assumed to be proportional to the neutron level at a time $(t - \tau)$ previously. The symbol τ represents the delay time. It will be shown later that for the conditions considered for this investigation this delay time is negligible, but for generality the equations will be derived with the lag time included. The coupling function between cores was assumed to be

$$f(n_1) = \frac{\alpha\, n_2(t - \tau)}{\ell} \qquad (3)$$

where

$n_2(t - \tau)$ = average neutron density in opposite slab a time $(t - \tau)$ previously, neutrons/cm^3

α = coupling coefficient

ℓ = neutron lifetime, sec.

The coupling coefficient, α, can be thought of as an equivalent reactivity since it is determined in terms of an equivalent δK for a region. The method used for determining the numerical value of α will be discussed in a later section.

The modified reactor kinetic equation for region one becomes

$$\frac{dn_1}{dt} = (\delta K)_1 \frac{n_1}{\ell} - \frac{\beta n_1}{\ell} + \sum_{i=1}^{6} \lambda_i c_i + \frac{\alpha n_2}{\ell} (t - \tau). \quad (4)$$

It was assumed that ℓ, λ_i, β and α were the same for each core. The equation for region two is identical to Equation 4 with the subscripts interchanged. Figure 2 presents a sketch of the reactor model used in this development.

An expression for $n(t - \tau)$ was derived as follows. It was assumed that the variation in neutron level with time is as shown in Figure 3 and $n(t - \tau)$ expanded in a series, the first two terms being

$$n(t - \tau) = n(t) - \frac{dn}{dt} \tau. \quad (5)$$

In Figure 3, $n(t)$ is the neutron density at time t, $n(t - \tau)$ is the neutron density at time $(t - \tau)$, and dn/dt is the rate of change of neutron density with time which was assumed to

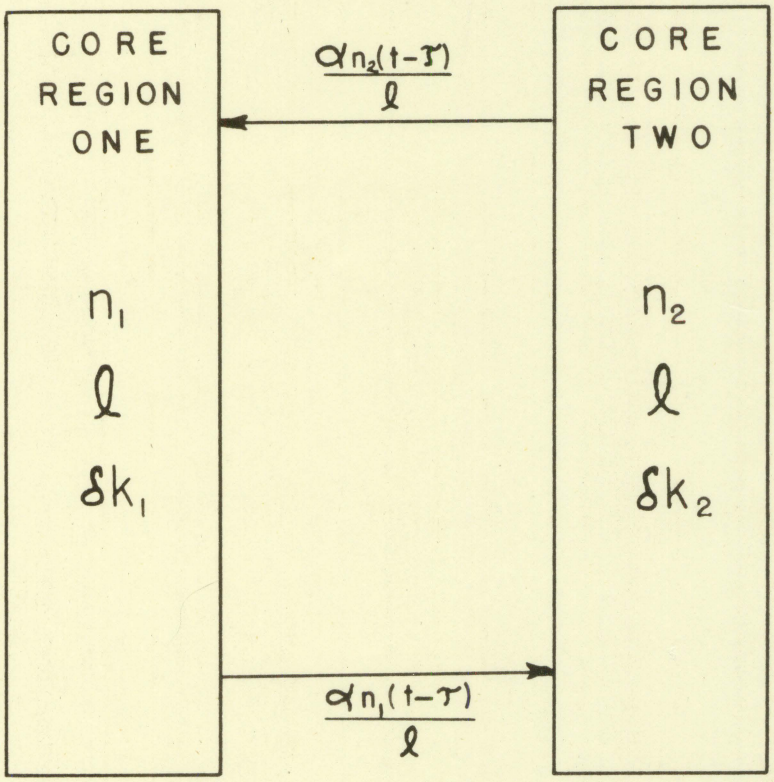

Figure 2. Reactor model

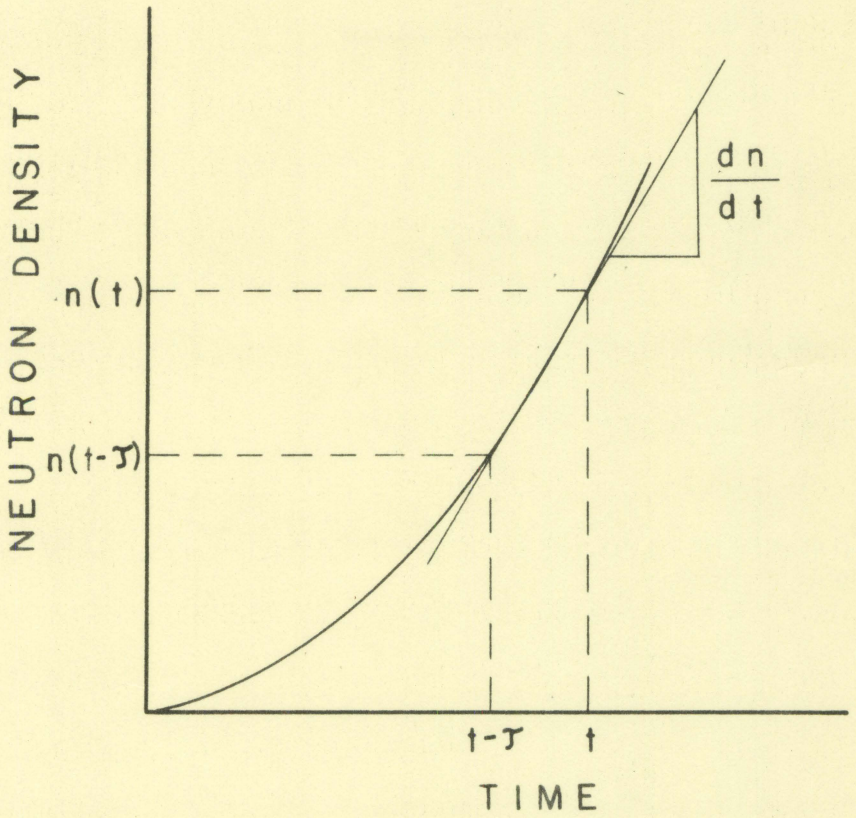

Figure 3. Assumed time variation of the neutron density used in deriving Equation 5

be constant over the time interval τ. It will be shown later that τ is of the order of 10^{-4} seconds, therefore higher order terms in Equation 5 should be unimportant.

Substitution of Equation 5 into Equation 4 yields the final modified reactor kinetic equations for the two regions

$$\frac{dn_1}{dt} = (\delta K)_1 \frac{n_1}{\ell} - \frac{\beta n_1}{\ell} + \sum_{i=1}^{6} \lambda_i c_{i_1} + \frac{\alpha n_2}{\ell} - \frac{\alpha}{\ell}\frac{dn_2}{dt}\tau \quad (6)$$

and

$$\frac{dn_2}{dt} = (\delta K)_2 \frac{n_2}{\ell} - \frac{\beta n_2}{\ell} + \sum_{i=1}^{6} \lambda_i c_{i2} + \frac{\alpha n_1}{\ell} - \frac{\alpha}{\ell}\frac{dn_1}{dt}\tau. \quad (7)$$

The differential equations for the delayed neutron precursors for the two regions are

$$\frac{dc_{i1}}{dt} = \frac{\beta_i n_1}{\ell} - \lambda_i c_{i1} \quad (8)$$

and

$$\frac{dc_{i2}}{dt} = \frac{\beta_i n_2}{\ell} - \lambda_i c_{i2} . \quad (9)$$

The inseparability of space and time variations of neutron flux is evident by the inclusion of the terms in Equations 6 and 7 which depends on the neutron flux shape across the reactor.

PROGRAMING KINETIC EQUATIONS FOR USE ON THE ANALOG COMPUTER

The details of the scaling of the reactor kinetic equations for solution on the analog computer are presented in this section. The general methods used in setting up the problems on the computer and some of the problems encountered are also outlined.

Scaling of Equations

For purposes of this work it was assumed that the delayed neutrons could be combined into one group having an average decay constant, λ, and a total fractional yield, β. Then c_i becomes c, the concentration of all of the precursors. With this assumption, Equations 6 and 8 become

$$\frac{dn_1}{dt} = (\delta K)_1 \frac{n_1}{\ell} - \frac{\beta n_1}{\ell} + \lambda c_1 + \frac{\alpha n_2}{\ell} - \frac{\alpha}{\ell} \frac{dn_2}{dt} \tau \qquad (10)$$

$$\frac{dc_1}{dt} = \frac{\beta n_1}{\ell} - \lambda c_1 . \qquad (11)$$

With this same substition Equations 7 and 9 become identical to Equations 10 and 11 with subscripts reversed. The values of ℓ, β and λ used in this study were

$$\ell = 1.35 \times 10^{-4} \text{ sec}$$

$$\beta = 0.00650$$

and $$\lambda = 0.0800 \quad \text{sec}^{-1}.$$

The value of β used was that given by Keppin and Wimett (21).

The method of scaling used followed the procedure presented by Korn and Korn (22). In this method the dependent variables appearing in the differential equations are rewritten in terms of machine units, one machine unit being 100 volts. The relationships between machine units and the actual dependent variables are

$$N = a_n n \tag{12}$$

$$C = a_c c \tag{13}$$

where capital letters represent the machine variables and the small letters represent the actual dependent variables. The scale factors a_n and a_c are found by dividing the maximum number of machine units expected from an amplifier by the maximum expected values of n or c. Since the maximum voltage output from an amplifier is 100 volts or one machine unit, a_n and a_c are given by

$$a_n = \frac{1}{n_{maximum}} \tag{14}$$

$$a_c = \frac{1}{c_{maximum}} . \tag{15}$$

For this work the maximum value of n was found by assuming that the maximum average neutron flux in a core region would be 2.20×10^{11} nv. Using a thermal neutron velocity of 2.20×10^{5} cm/sec, the maximum value of n was

$$n_{maximum} = \frac{\phi}{v} = \frac{2.2 \times 10^{11}}{2.2 \times 10^{5}} \tag{16}$$

$$= 10^6 \frac{\text{neutrons}}{\text{cm}^3} .$$

The maximum value of c, the delayed neutron precursor concentration, was determined from Equation 11 considering equilibrium conditions. Substituting numerical values for ℓ, β and λ into Equation 11 and setting dc/dt = 0, the value of c was

$$c = \frac{\beta n}{\ell \lambda} = \frac{(0.00650)n}{(1.35 \times 10^{-4})(0.0800)}$$

$$= 600n . \qquad (17)$$

Substitution of the maximum value of n from Equation 16 into this expression for c gave

$$c_{maximum} = 6.00 \times 10^8 \frac{\text{precursors}}{\text{cm}^3} .$$

The scale factors a_n and a_c were therefore

$$a_n = \frac{1}{10^6}$$

and

$$a_c = \frac{1}{6.00} \times 10^8 .$$

The relationships between the real independent variables and machine variables were

$$n = 10^6 N \qquad (18)$$

and

$$c = 6.00 \times 10^8 C . \qquad (19)$$

The lag time, τ, which represents the time required for a change in the neutron flux in one slab to be reflected in

the kinetic behavior of the opposite region was assumed, as by Baldwin (4), to be equal to the time required for a thermal neutron to traverse the separation distance between slabs. This distance in the UTR-10 is approximately 18 inches. Therefore, for a thermal neutron velocity of 2.20×10^5 cm/sec, the value of τ is

$$= \frac{(18.0)(2.54)}{2.20 \times 10^5} = 2.10 \times 10^{-4} \text{ sec} .$$

It would probably be more nearly correct to assume that the lag time, τ, corresponds to the time required for a neutron wave to travel the separation distance between cores. Uhrig[1] has shown that for the frequencies of interest this time is approximately ten times the value calculated using the velocity of thermal neutrons. In either case this delay time is significant only for very short reactor periods.

Equations 10 and 11 were rewritten in terms of machine variables. Substitution of the values of β, ℓ, λ and τ resulted in the following equations:

$$\frac{dN_1}{dt} = 7.40 \times 10^3 (\delta K)_1 N_1 - 48.1 N_1 + 48.0 C_1 + 7.40 \times 10^3 \alpha N_2 - 1.55 \frac{\alpha dN_2}{dt} \qquad (20)$$

$$\frac{dC_1}{dt} = 0.0803 N_1 - 0.0800 C_1 \qquad (21)$$

---

[1] Uhrig, Robert E., Ames, Iowa. Evaluation of subcritical assembly characteristics from neutron wave characteristics. Private communication. 1960.

These equations are in terms of real time, that is, no time scaling was used.

It was found that the term containing the lag time, τ, could be neglected when compared with the other terms in Equation 20. This can be demonstrated by considering the magnitude of the last term in Equation 20 when the reactor period is ten seconds and N_1 is equal to one machine unit. It was felt that a period of ten seconds would be the smallest period that would be of interest in this work and a value of N_1 of one machine unit is the maximum output from an amplifier. The reactor period as defined by Schultz (29) is

$$\text{Period} = \frac{n}{\frac{dn}{dt}} \qquad (22)$$

therefore dn/dt for these conditions becomes

$$dn/dt = 0.100 \text{ sec}^{-1} .$$

Since α in all cases considered is of the same order of magnitude as δK, it can be seen by comparing terms in Equations 20 that the term containing τ is much smaller than any other. The last term was therefore dropped from the equations.

The equations which were solved on the analog computer were

$$\frac{dN_1}{dt} = 7.40\text{x}10^{3}(\delta K)_1 N_1 - 48.1 N_1 + 48.0 C_1 + 7.40\text{x}10^{-3}\alpha N_2 \qquad (23)$$

$$\frac{dN_2}{dt} = 7.40\text{x}10^{3}(\delta K)_2 N_2 - 48.1 N_2 + 48.0 C_2 + 7.40\text{x}10^{-3}\alpha N_1 \qquad (24)$$

$$\frac{dC_1}{dt} = 0.0803N_1 - 0.0800C_1 \qquad (25)$$

$$\frac{dC_2}{dt} = 0.0803N_2 - 0.0800C_2 \, . \qquad (26)$$

Step Inputs of Reactivity

The response of the system to step inputs of reactivity was the first case studied. This work was performed for a range of values of δK for each region and for several values of α. The values of α and the range of values of reactivity for each region used in each run are listed in Table 1.

Table 1. Values of parameters used in step input study

Run designation	Coupling α	Range of $(\delta K)_1$	Range of $(\delta K)_2$
B	0.00500	+0.00240 to -0.00165	-0.0107 to -0.0304
C	0.0100	-0.000500 to -0.0140	-0.00695 to -0.0278
D	0.0150	-0.00425 to -0.0218	-0.0106 to -0.0304
E	0.020	-0.00915 to -0.0240	-0.0156 to -0.0304
F	0.040	-0.0229 to -0.0790	-0.0212 to -0.0610
G	0.060	-0.0320 to -0.0750	-0.0460 to -0.100
H	0.100	-0.0739 to -0.115	-0.0870 to -0.130

In all of the cases studied it was assumed that the temperature coefficient of reactivity of the reactor was zero.

In most of the runs, the individual reactivity term of each slab was negative. The only exceptions were in run B

in which case, due to the small value of coupling, several of the reactivity terms were positive.

A total of eight amplifiers were required for solving Equations 23, 24, 25 and 26. The wiring diagrams used are shown in Figure 4. The multiplication of δK times N was performed using the ten turn potentiometers which are provided on the computer. The value of δK by which N was multiplied should have been proportional to the potentiometer setting. It was found however that the actual output from these potentiometers was not linear with the dial setting due to circuit loading; therefore a calibration curve was determined for each potentiometer and used for converting dial readings to δK.

The values of components and potentiometer settings are listed in Table 6 in Appendix C.

The general procedures used during computer operation were as follows:

(1) The desired value of α was established by adjusting potentiometers 12A and 13B.

(2) The values of $(\delta K)_1$ and $(\delta K)_2$ were established by setting the two ten turn potentiometers.

(3) The initial conditions were set on amplifiers 2, 3, 8, and 9. The initial conditions of N_1 and N_2 were established by arbitrarily picking one tenth of a machine unit or ten volts as the starting

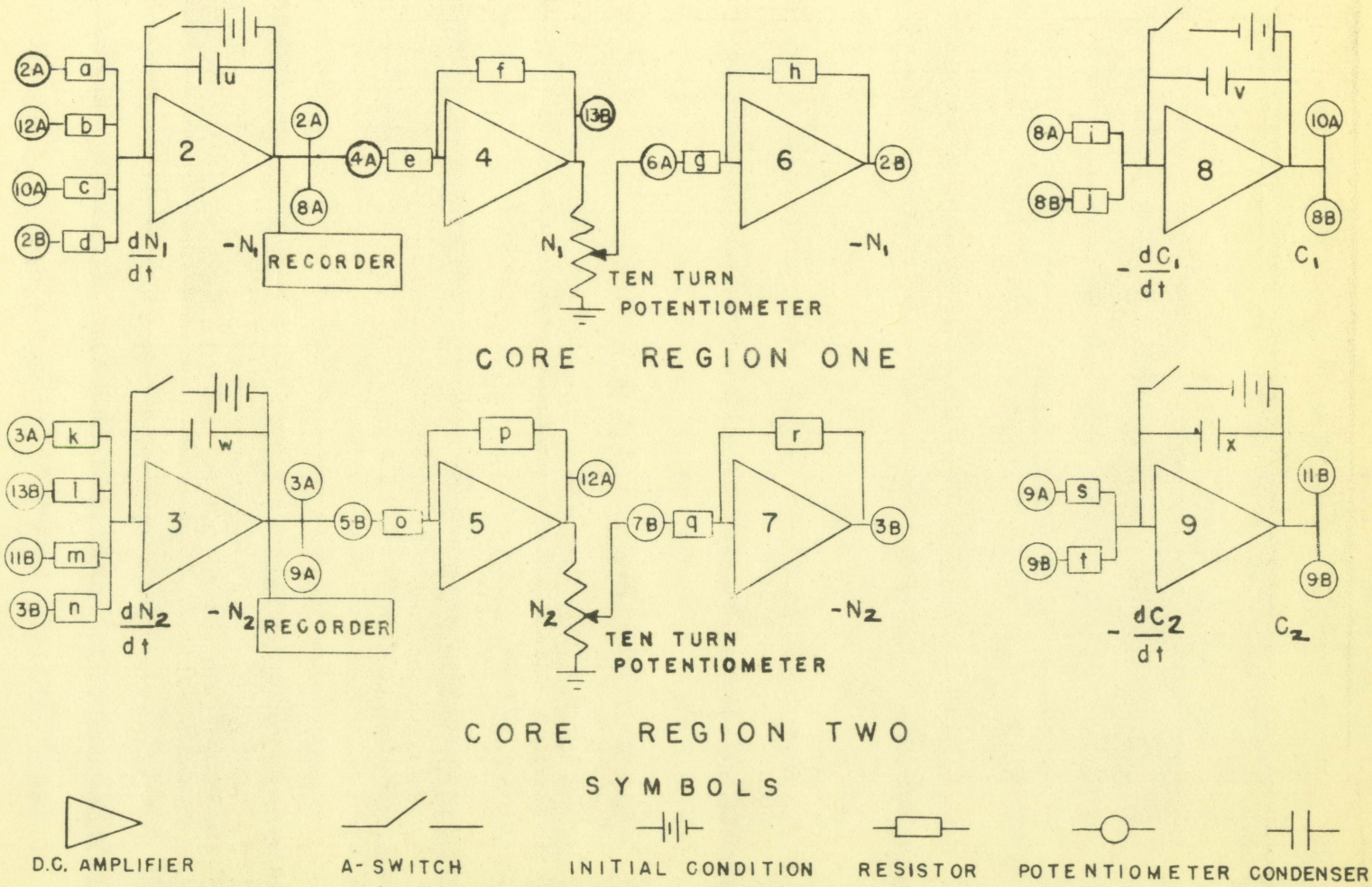

Figure 4. Wiring diagrams for step inputs of reactivity

level. The initial conditions of C_1 and C_2 were determined from Equations 25 and 26 for equilibrium conditions. The initial conditions of N_1 and N_2 were usually set for N_1 equal to N_2.

(4) The manual starting switch, the A switch, was opened thereby starting the problem.

(5) The signals from aplifier 2 and 3 were recorded on a two channel Brush recorder.

(6) The problem was allowed to run until the output from amplifiers 2 and 3 approached 80 volts.

(7) The A switch was closed stopping the problem.

The reactivity term for region 2, δK_2, was held constant and δK_1 was varied over a range of values until reactor periods from 15 to 100 seconds were obtained. δK_2 was then reset to a different value and the above procedure repeated.

The items of primary interest in this problem were the asymptotic periods for each slab and the relationship between N_1 and N_2 after the initial transients due to the step inputs of reactivity had disappeared.

It was found that to obtain constant reactor periods and constant relationships between N_1 and N_2 it was necessary to make a trial run for each condition studied. From this trial run, the ratio of N_1 to N_2 after the transients had died out was established. The initial conditions on amplifiers 2, 3, 8, and 9 were then reset to correspond to this ratio. Re-

setting the initial conditions to these new values was equivalent to changing ranges, and it was found that during the second trial the asymptotic periods for both slabs were the same and the ratio of N_1 to N_2 remained approximately constant.

Sinusoidal Variations of the Coupling Constant

The second phase of the study was the determination of the response of the reactor to a sinusoidal variation of the coupling between regions. The sinusoidal variation used was of the form

$$\alpha = \alpha_o + \alpha_t \sin\omega t \qquad (27)$$

where

α_o = steady state coupling term

α_t = amplitude of sinusoidal component of the coupling.

The values of α_o, α_t and the ratio of N_1 to N_2 used for each run are shown in Table 2.

Table 2. Values of parameters used in the sinusoidal variation of coupling

Run designation	N_{10}/N_{20}	α_o	Range of α_t	Maximum frequency used
I-L	1.00	0.0135	0.00100 to 0.000300	1.00 cps
M	1.00	0.0155	0.00100 to 0.000300	20.0 cps
O	1.00	0.0175	0.00100 to 0.000300	1.00 cps
P	1.00	0.0200	0.00100 to 0.000300	1.00 cps
Q	1.20	0.0155	0.00100 to 0.000300	20.0 cps

The form of α assumed for this work would approximate that which would be obtained with a reactivity oscillator placed in the graphite region between the core tanks. It is visualized that this oscillator would consist of a rotating cadmium pattern which would have the effect of varying the reactivity coupling between slabs in a sinusoidal manner about some steady state value.

With the introduction of α as a function of time, Equations 23 and 24 no longer have constant coefficients. The two expressions containing αN_1 and αN_2 involve the multiplication of two terms which are both functions of time. Therefore, the mechanical servo-multipliers were used to obtain these products.

The additions to the circuits required to do this are shown in Figure 5. The expression for α was broken up into two terms; the product $\alpha_o N_1$ and $\alpha_o N_2$ being obtained as in the step input case, and the expressions $\alpha_t N_1 \sin wt$ and $\alpha_t N_2 \sin wt$ being obtained from the servo-multiplier. The values of components and potentiometer settings are given in Table 7 in Appendix C.

It was desired to obtain the response of the system to frequencies of oscillation varying from 0.01 cycles per second to about 20 cycles per second. The response of the mechanical multipliers used was limited to about 1 cycle per second so it was therefore necessary to time scale the reactor kinetic

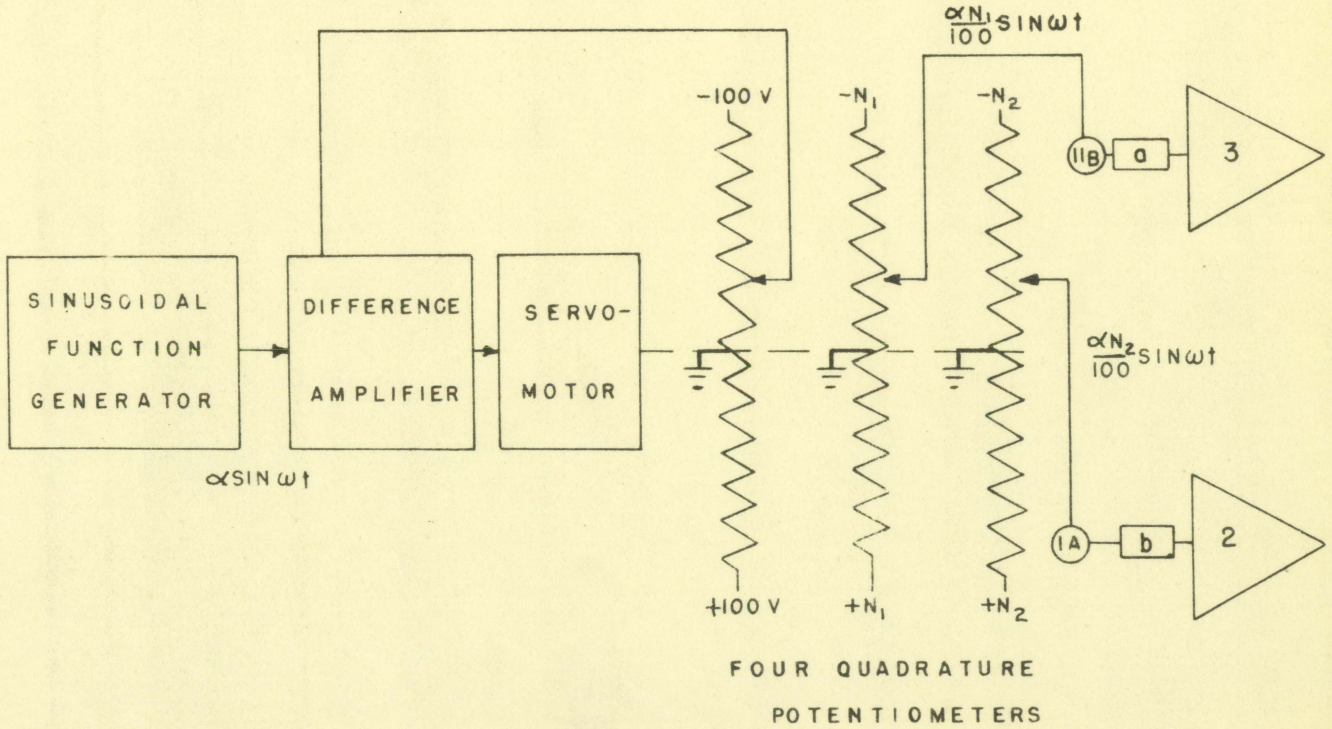

Figure 5. Additions to computer to obtain sinusoidal variations of coupling

equations to obtain the response of the reactor system to frequencies above 1 cycle per second. The time scaling used had to be such that the analog computer solution was slowed down in time. The relationship between computer time and real time was chosen as

$$\tau = 20t \tag{28}$$

where

τ = computer time

t = real time.

The relationship between derivatives in real time and computer time is

$$\frac{d(\ )}{dt} = \frac{d(\ )}{d\tau}\frac{d\tau}{dt}. \tag{29}$$

For this case

$$\frac{d\tau}{dt} = 20 \tag{30}$$

and therefore

$$\frac{d(\ )}{dt} = 20\,\frac{d(\ )}{d\tau}. \tag{31}$$

Substitution of Equation 31 into Equations 23, 24, 25 and 26 yields

$$\frac{dN_1}{d\tau} = 370N_1(\delta K)_1 - 2.41N_1 + 2.40C_1 + 370\alpha N_2 \tag{32}$$

$$\frac{dN_2}{d\tau} = 370N_2(\delta K)_2 - 2.41N_2 + 2.40C_2 + 370\alpha N_1 \tag{33}$$

$$\frac{dC_1}{d\tau} = 0.00401N_1 - 0.00400C_1 \tag{34}$$

$$\frac{dC_2}{d\tau} = 0.00401N_2 - 0.00400C_2 \quad . \tag{35}$$

It can be seen from Table 2 that runs I, J, K, L, O, and P were carried out to one cycle per second but runs M and Q were taken to twenty cycles per second. The time scaled equations were used for the latter two cases only.

The value of the steady state coupling term ($\alpha_o = 0.0155$) used in runs M and Q is the value that has been determined for the UTR-10. This value of α_o was determined by considering the decrease in reactivity of one slab if all of the fuel is removed from the opposite region and replaced by graphite. The extra fuel required to make the single slab critical can be related to the equivalent reactivity contributed by the other region from[1]

$$\frac{\frac{\delta K}{K}}{\frac{\Delta M}{M}} = 0.336 \tag{36}$$

where

ΔM = increase in fuel

M = original critical mass.

This equivalent reactivity is equal to the coupling coefficient α used in this work. Inherent in this is the assumption that reactivity ($\delta K/K$) can be used interchangeably

---

[1]Crews, Ray F. Mountain View, California. Private communication to Dr. Glenn Murphy. 1959.

with δK since α, the coupling constant, is an equivalent δK rather than $\delta K/K$. This assumption is valid if K_{eff} is approximately equal to one.

The values of the time dependent coupling term, α_t, chosen for this study were based on work at Argonne National Laboratory (5). This seemed to be a reasonable range of values for the amplitude of oscillation of coupling that might be obtained from a reactivity oscillator placed in the graphite between cores.

Ramp Inputs of Reactivity

The response of the reactor to a ramp input of reactivity into one of the core regions was the third case considered. The form of the input used was

$$\delta K = (\delta K)_o + \gamma t \qquad (37)$$

where

$(\delta K)_o$ = initial reactivity of the region

γ = rate of reactivity input, $\delta K/sec^{-1}$

t = time, sec.

This form of reactivity input corresponds over the linear range of δK versus rod position to the case when a control rod is withdrawn from the reactor. By adjusting the term δK_o the rod withdrawal can be started with the reactor critical or subcritical; both cases were considered here.

The UTR-10 has four rods: two safety rods, one shim rod

and one regulating rod. However, the start-up sequence is interlocked so that the two safety rods must be completely withdrawn from the core before either the shim or regulating rod can be moved; that is, only the shim and regulating rods can be moved when the reactor is critical or near critical. For this reason the rod withdrawal rates and total rod worths considered in this work were those for the regulating rod and the shim rod (2). The data for these rods are listed in Table 3. The primary item of interest in this study was the

Table 3. Shim and regulating rod data

Control rod	Maximum reactivity input rate	Total worth
Regulating	0.000100/sec	0.00200
Shim	0.000450/sec	0.00800

determination of the effect of flux tilting on rod effectiveness. The degree of flux tilting at the time rod withdrawal is started is determined by the value of δK_o for the region from which the rod is being withdrawn and also the value of δK for the opposite region.

To study this effect it was necessary to solve the reactor kinetic equations for the required reactivity values for each slab for various ratios of N_1 to N_2. This was done for just critical conditions. The methods used for solving the equations are presented in Appendix A. The initial condi-

tions on amplifiers 2, 3, 8, and 9 were then set to correspond to the ratios of N_1 to N_2 obtained.

Introducing the reactivity as a function of time results in kinetic equations which contain terms which do not have constant coefficients. It is therefore necessary to use the servo-multipliers again to obtain the product δK_1 times N_1. This product was divided into two terms; $(\delta K)_o N_1$ which was obtained by using the ten turn potentiometer; and $\gamma t N_1$ which was obtained from the servo-multiplier. The term $(\delta K)_2 N_2$ (δK_2 was constant) was also obtained by using the ten turn potentiometer. The additions to the wiring diagram for this work are shown in Figure 6. Component values and potentiometer setting are given in Table 8, Appendix C.

An integrating amplifier was used to generate the ramp input signal which was fed to the servo-multiplier difference amplifier. The amplification factor on the integrating amplifier was adjusted to give the desired reactivity input rate.

For the cases in which the ramp input was started with the reactor subcritical a source term was included in Equations 23 and 24.

The coupling term was held constant at 0.0155 for all of these studies. The values of $(\delta K)_o$, $(\delta K)_2$, γ and the ratio of N_1 to N_2 for each run are listed in Table 4.

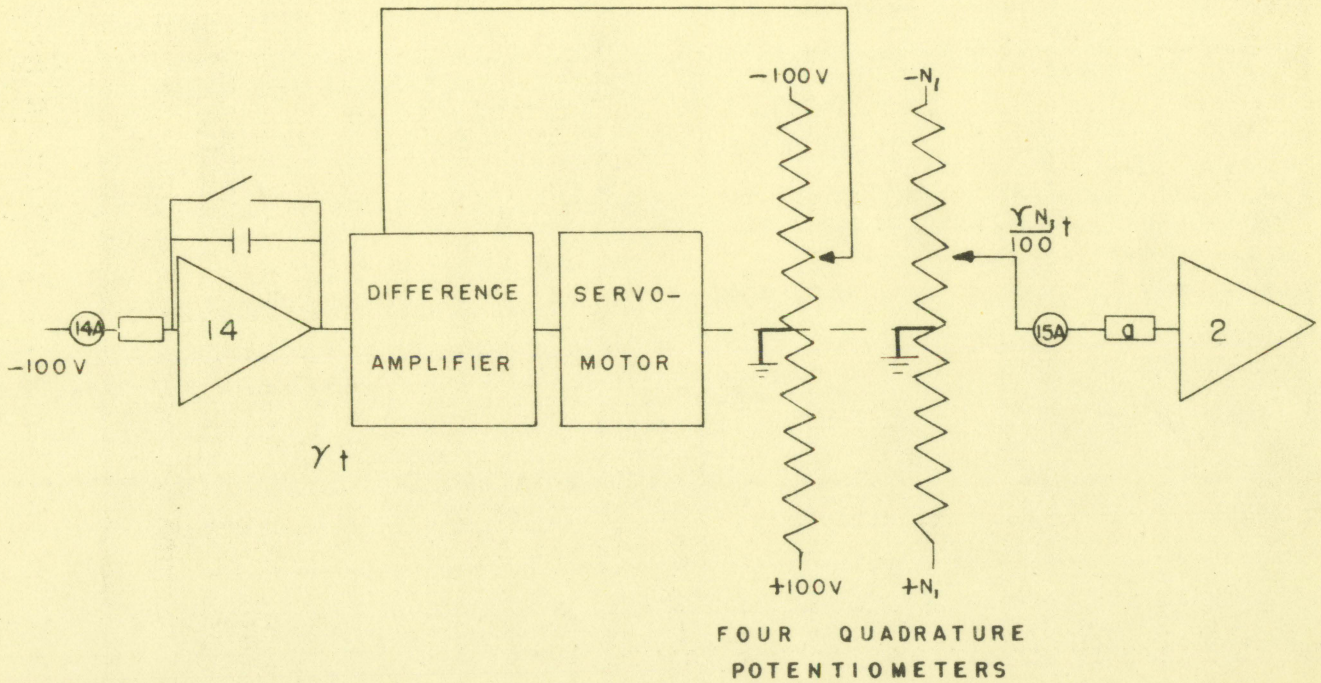

Figure 6. Additions to the computer to obtain a ramp input of reactivity

Table 4. Parameters used in ramp input

Run designation	Reactivity input rate (δK)/sec	Source term	Reactor condition	Range of $(\delta K)_{1-0}$	Range of $(\delta K)_{2-0}$	$(N_1/N_2)_0$
B (1-6)	0.000100	0	critical	-0.00780 to -0.0310	-0.0078 to -0.0310	0.500 to 2.00
C (1-6)	0.000100	0.300 machine units	sub-critical	-0.00800 to -0.0318	-0.00800 to -0.0318	0.500 to 2.00
D (1-6)	0.000100	0.300 machine units	sub-critical	-0.00850 to -0.0337	-0.00850 to -0.0337	0.500 to 2.00
E (1-5)	0.00045	0.300 machine units	sub-critical	-0.00850 to -0.0337	-0.00850 to -0.0337	0.500 to 2.00
F (1-6)	0.00045	0.300 machine units	sub-critical	-0.00800 to -0.0318	-0.00800 to -0.0318	0.500 to 2.00
G (1-6)	0.00045	0	critical	-0.0078 to -0.0310	-0.0078 to -0.0310	0.500 to 2.00

Ramp Input with Sinusoidal Variations of Coupling

The response of the reactor to a ramp input of reactivity with the reactivity oscillator running was investigated.

The same values of δK_0, δK_2, and γ that were used in the previous work were used here. The steady state coupling was held constant at 0.0155 and the amplitude of oscillation was fixed at 0.000500. This was done for several degrees of flux tilting and oscillator frequencies. The values of the parameters used for each run are listed in Table 5.

The computer wiring diagrams for this operation were the combined circuits used in the oscillator study, ramp study and step input case. A separate diagram for this is not shown.

Table 5. Parameter used in ramp plus sinusoidal input

Run designation	Frequency of oscillation	Other conditions
B (7-24)	0.0600 to 0.500 cps	Same as listed in Table 4
C (7-24)	0.0600 to 0.500 cps	Same as listed in Table 4
D (6&7)	0.500 cps	Same as listed in Table 4
E (6-20)	0.0600 to 0.500 cps	Same as listed in Table 4
F (7-27)	0.0600 to 1.00 cps	Same as listed in Table 4
G (7-29)	0.0600 to 1.00 cps	Same as listed in Table 4

ANALYSIS OF DATA AND PRESENTATION OF RESULTS

The data obtained during the investigation were in the form of recorder traces which showed the variations with time of the average neutron densities in the two regions of the reactor. The methods used in reducing these data are outlined in this section, and the final reduced data are presented in forms which are more meaningful than the original recorded results.

Step Inputs of Reactivity

The voltage signals from aplifiers 2 and 3 which corresponded to N_1 and N_2 respectively were recorded. Typical results, which are for runs 5D, 25D and 40D, are shown in Figure 7. In the case of run 5D the ratio of the step input of reactivity into region 1 to that into region 2 was such that the neutron flux was tilted with the high side in slab 1. This resulted in a ratio of N_1 to N_2 of 1.45. Run 25D illustrates the behavior with no flux tilting ($N_1 = N_2$), and run 40D illustrates the condition with the flux tilted in an opposite sense to that of run 5D.

The ratio of N_1 to N_2 and stable reactor period were taken from the computer traces. The reactor period was obtained from the following equation.

$$N = N_o e^{t-t_o/\tau} \qquad (38)$$

Figure 7. Typical computer results for step inputs of reactivity increasing time to the left

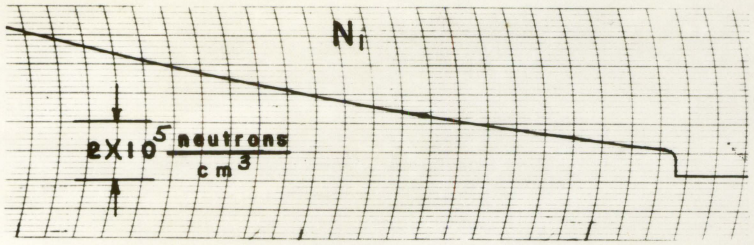
N_1
$2 \times 10^5 \frac{\text{neutrons}}{cm^3}$

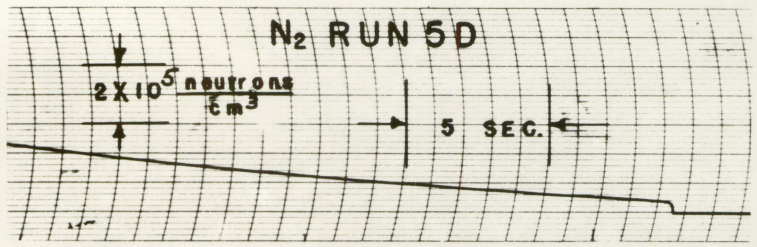
N_2 RUN 5D
$2 \times 10^5 \frac{\text{neutrons}}{cm^3}$
5 SEC.

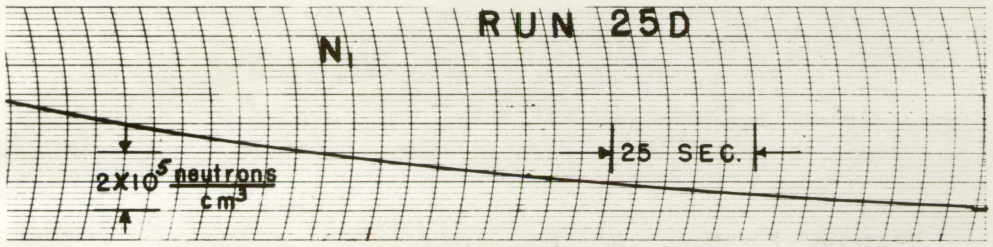
N_1
RUN 25D
$2 \times 10^5 \frac{\text{neutrons}}{cm^3}$
25 SEC.

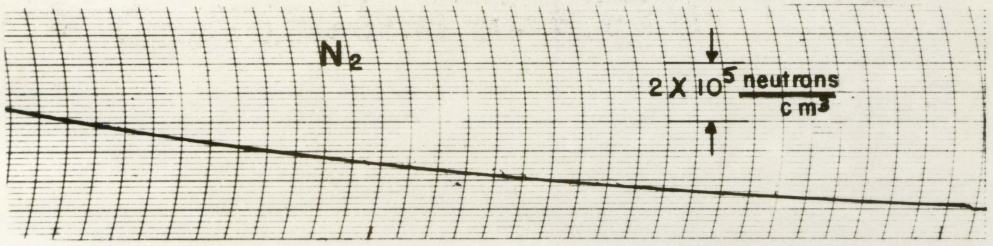
N_2
$2 \times 10^5 \frac{\text{neutrons}}{cm^3}$

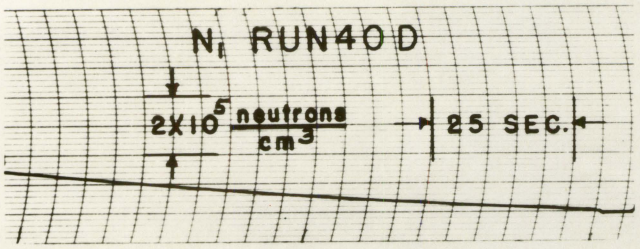
N_1 RUN 40D
$2 \times 10^5 \frac{\text{neutrons}}{cm^3}$
25 SEC.

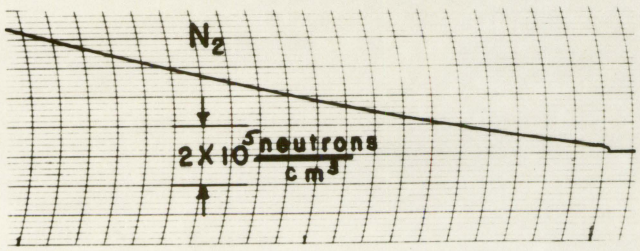
N_2
$2 \times 10^5 \frac{\text{neutrons}}{cm^3}$

where

N = neutron density at time, t

N_o = neutron density at time, t_o

τ = reactor period.

This relationship applies to the part of the curve where the reactor is on a stable period, and it was therefore necessary to pick N and N_o at points along the curve where this condition (purely exponential rise in power) existed. Since N and N_o were used as a ratio it was not necessary to convert machine variables to the actual variables. The ratio of N_1 to N_2 in the two slabs was obtained from the portions of the curve where the stable reactor period existed. Again, since a ratio was used, machine variables were used rather than the actual variables.

It was necessary to make several cross-plots of the original data to obtain the data required for plotting the final desired curves. The first curve consisted of a plot of reactor period versus δK_1 with δK_2 held constant as a parameter. A typical set of curves is shown in Figure 8. The data obtained from these curves were used to plot the constant period contour lines of Figures 11, 12, 13 and 14. Additional cross-plotting was required to obtain the necessary information for plotting the constant neutron density lines shown on these figures. The ratio of N_1 to N_2 was plotted versus reactor period with δK_2 held constant. A typical

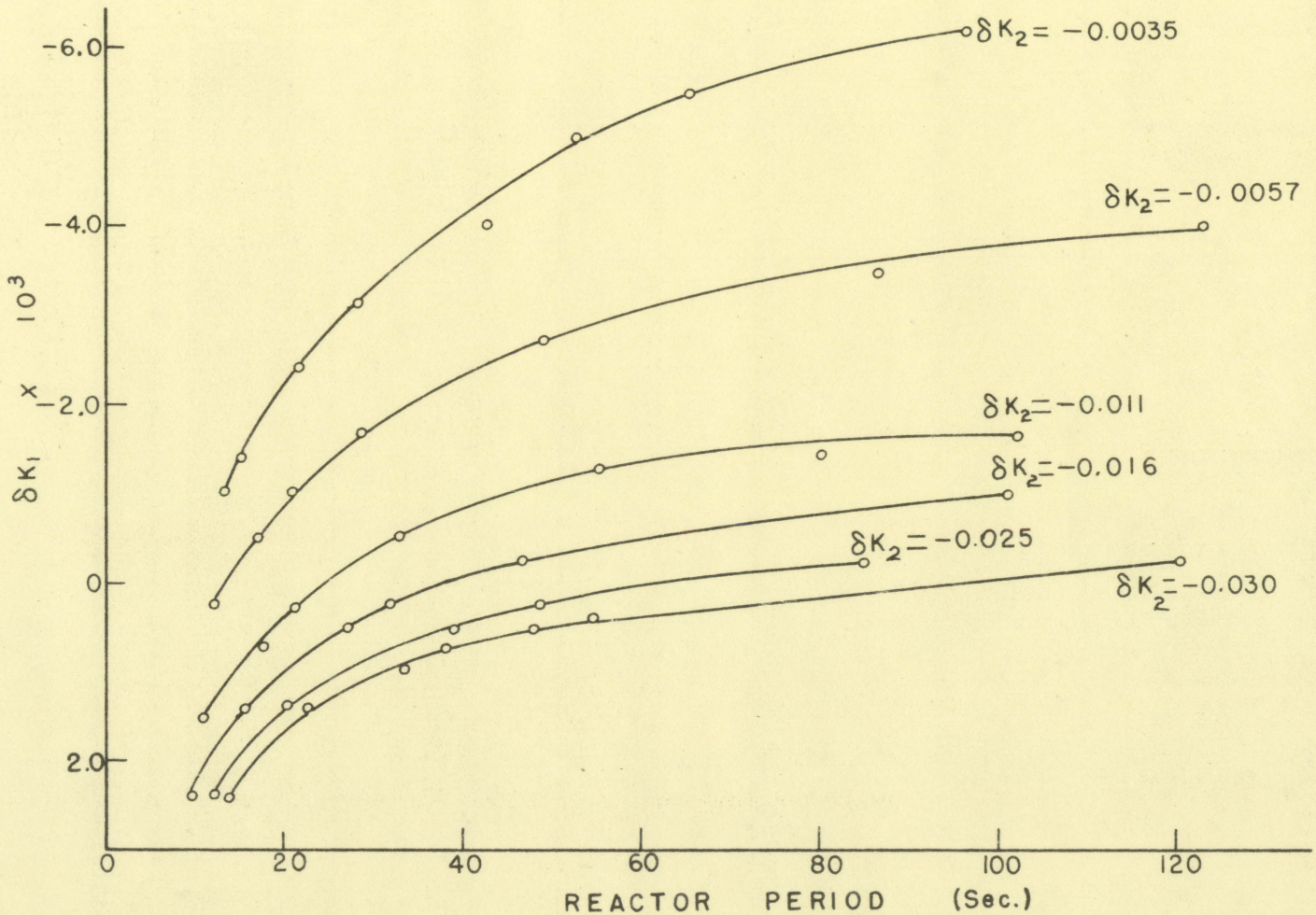

Figure 8. Reactor period versus reactivity for region one

set of curves is shown in Figure 9. The ratio of N_1 to N_2 was plotted versus δK_2 for constant reactor periods of 15 and 100 seconds. This is shown in Figure 10. These data were obtained from Figure 9. Using this latter set of curves it was then possible to pick off points of integral values of N_1/N_2 for points along the constant period lines. In summary, three different plots of the computer data were required to obtain the data needed to plot the curves of Figures 11, 12, 13 and 14.

In Figures 11, 12, 13 and 14 reactor period is shown as a function of δK_1 and δK_2. Each set of curves is for a constant value of the coupling constant. The curves shown are typical of those obtained from the cases studied. These curves show the effect of individual slab reactivity on the stable reactor period and also upon flux tilting.

Sinusoidal Variations of the Coupling Constant

Typical computer results, which were obtained from runs 45m and 38Q, are shown in Figure 15. Run 45m illustrates the behavior of the two regions with no flux tilting and run 38Q illustrates the behavior with the flux tilted so that the steady state value of N_1/N_2 was 1.20. The strip chart marked $\delta\alpha$ presents a record of the signal from the follow-up potentiometer of the servo-multiplier. This signal was proportional to the sinusoidal component of

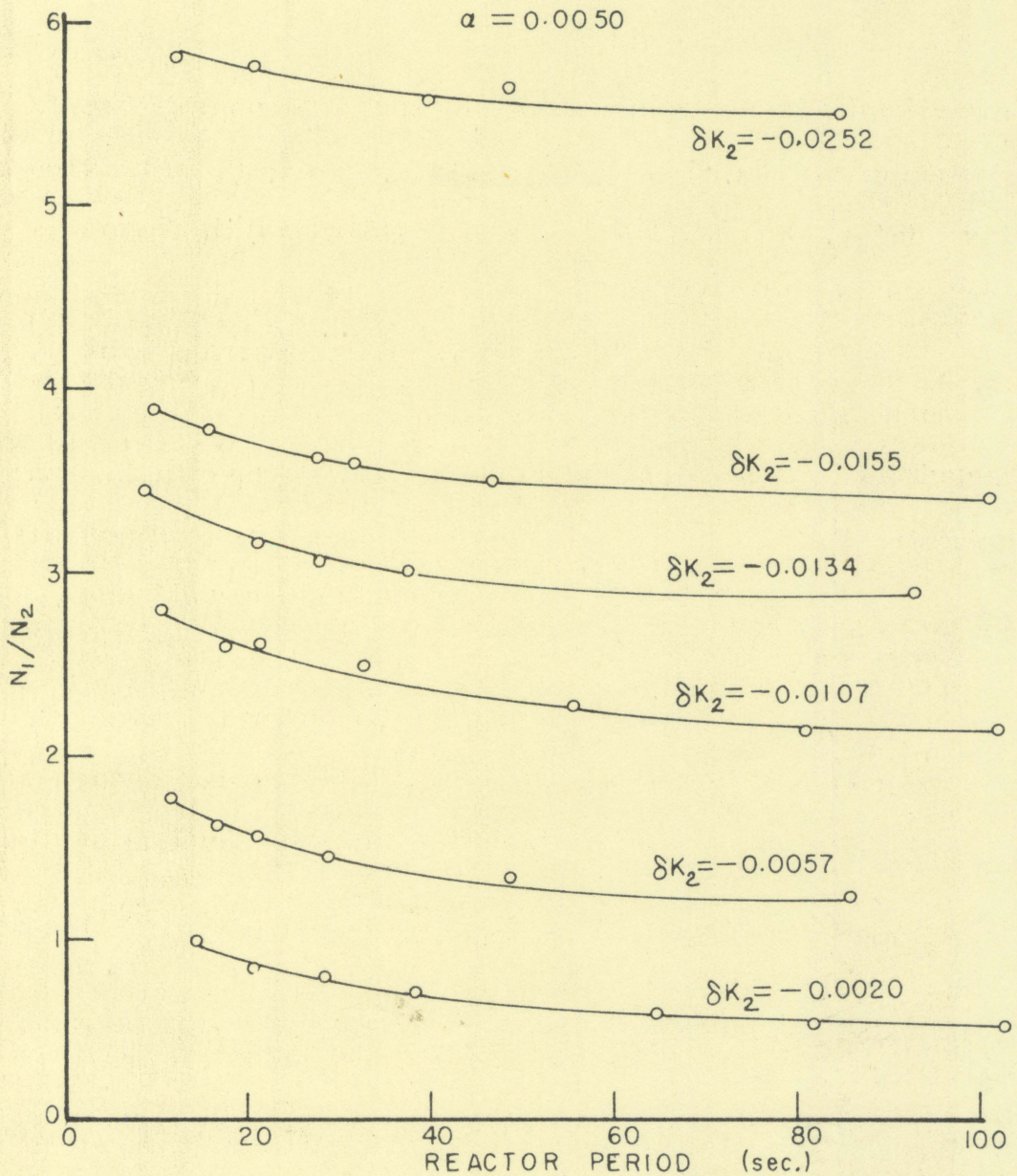

Figure 9. Neutron density ratio versus reactor period

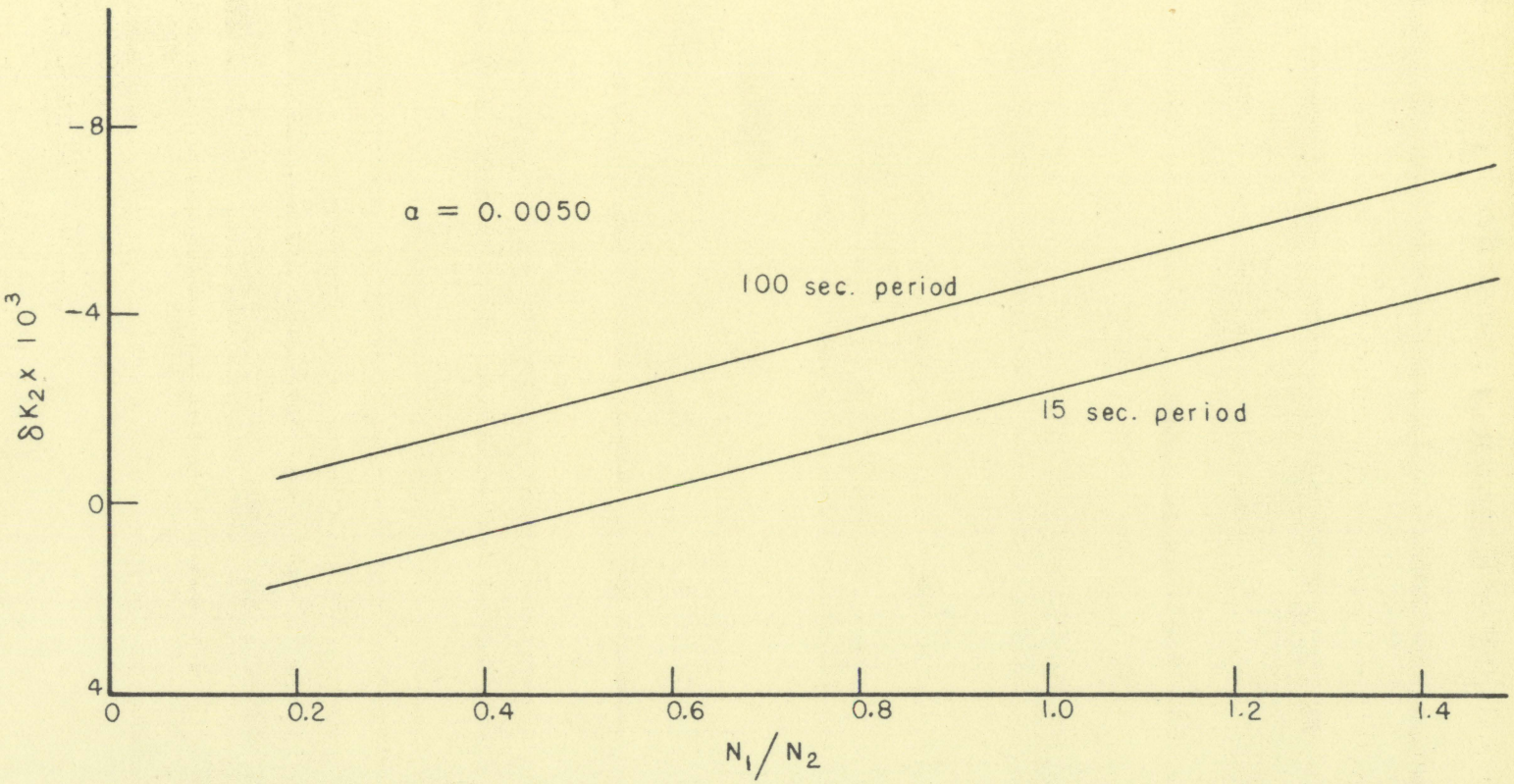

Figure 10. Reactivity of region two versus neutron density

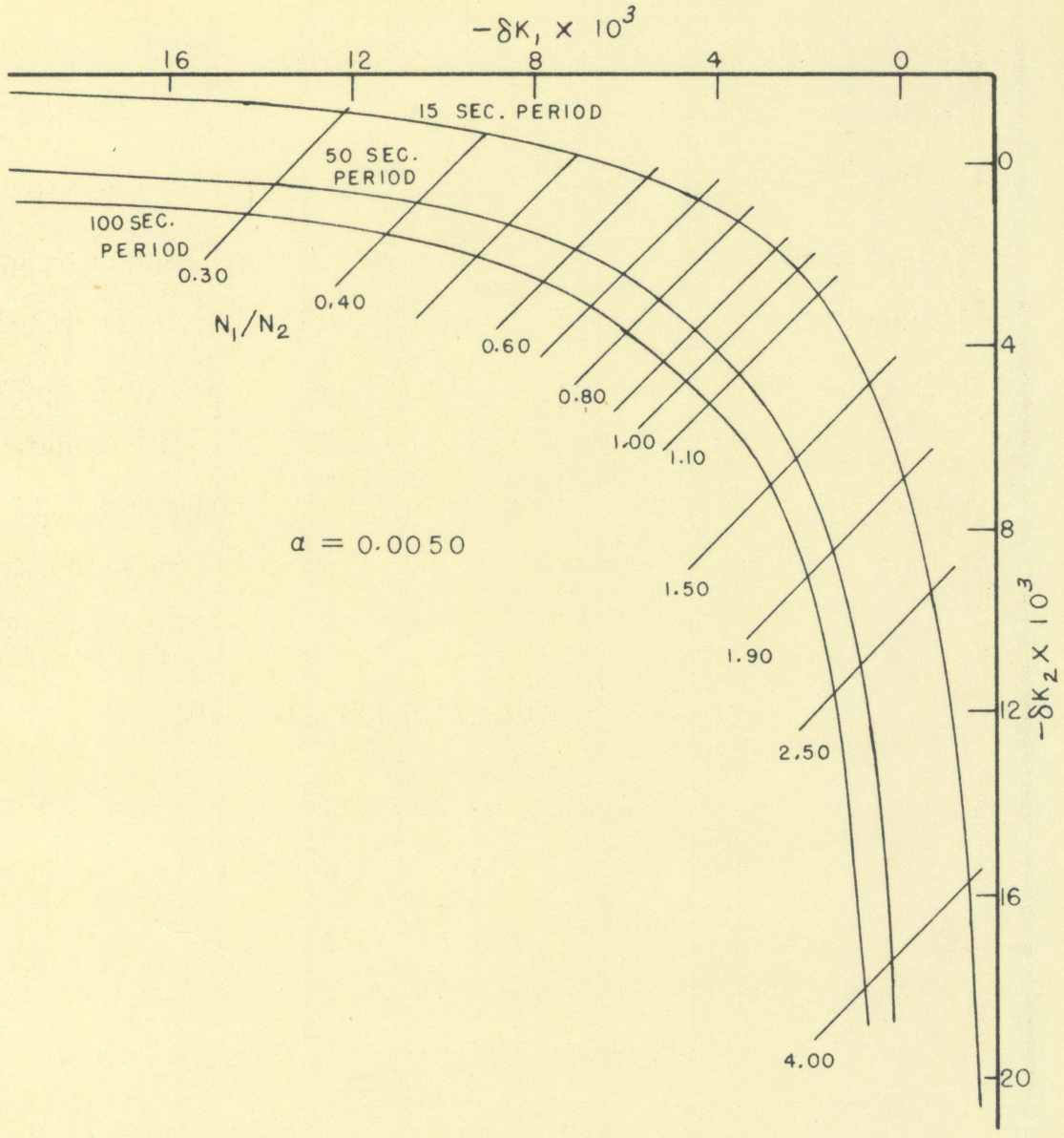

Figure 11. Reactor periods for various values of δK_1 and δK_2

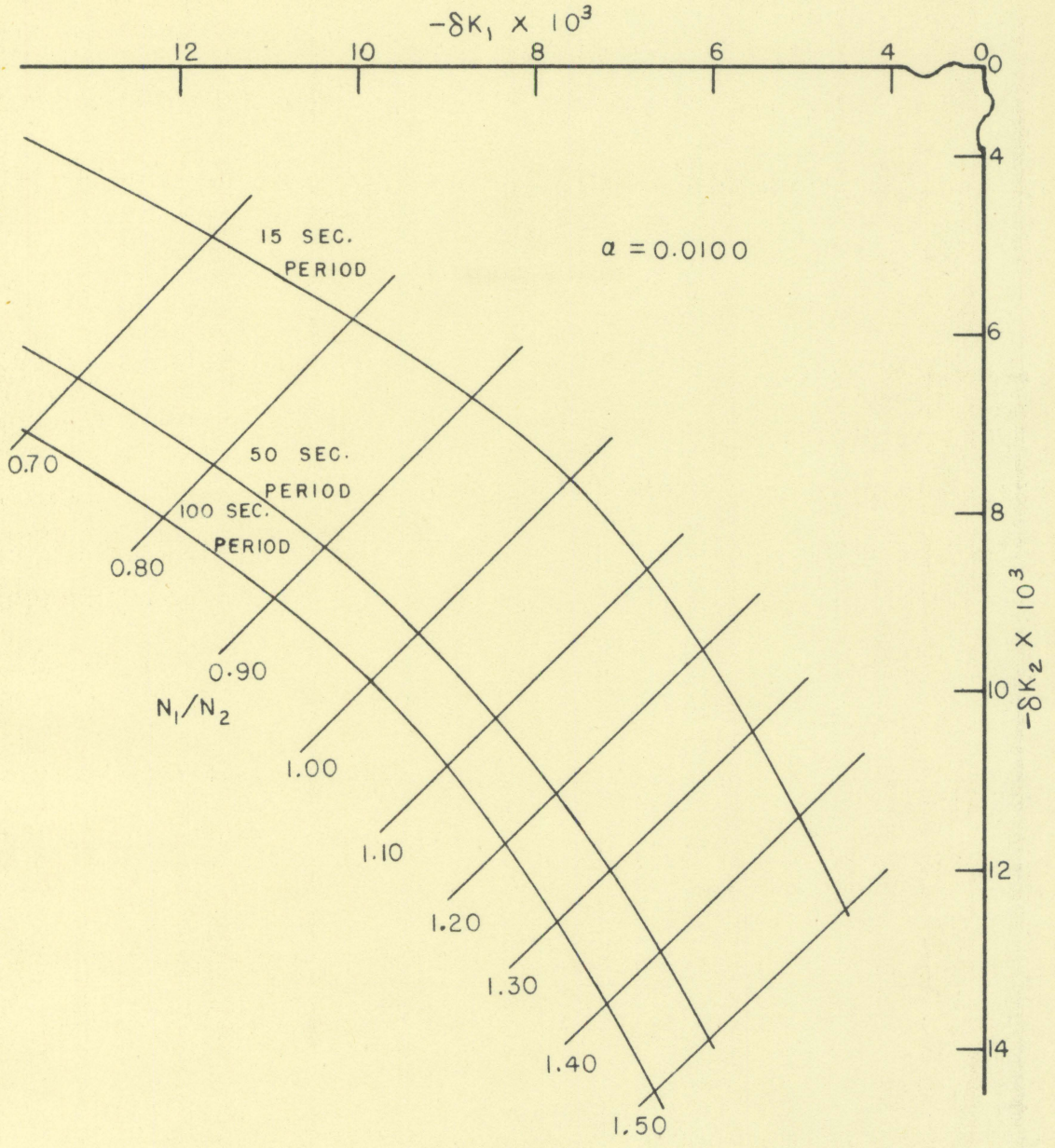

Figure 12. Reactor periods for various values of δK_1 and δK_2

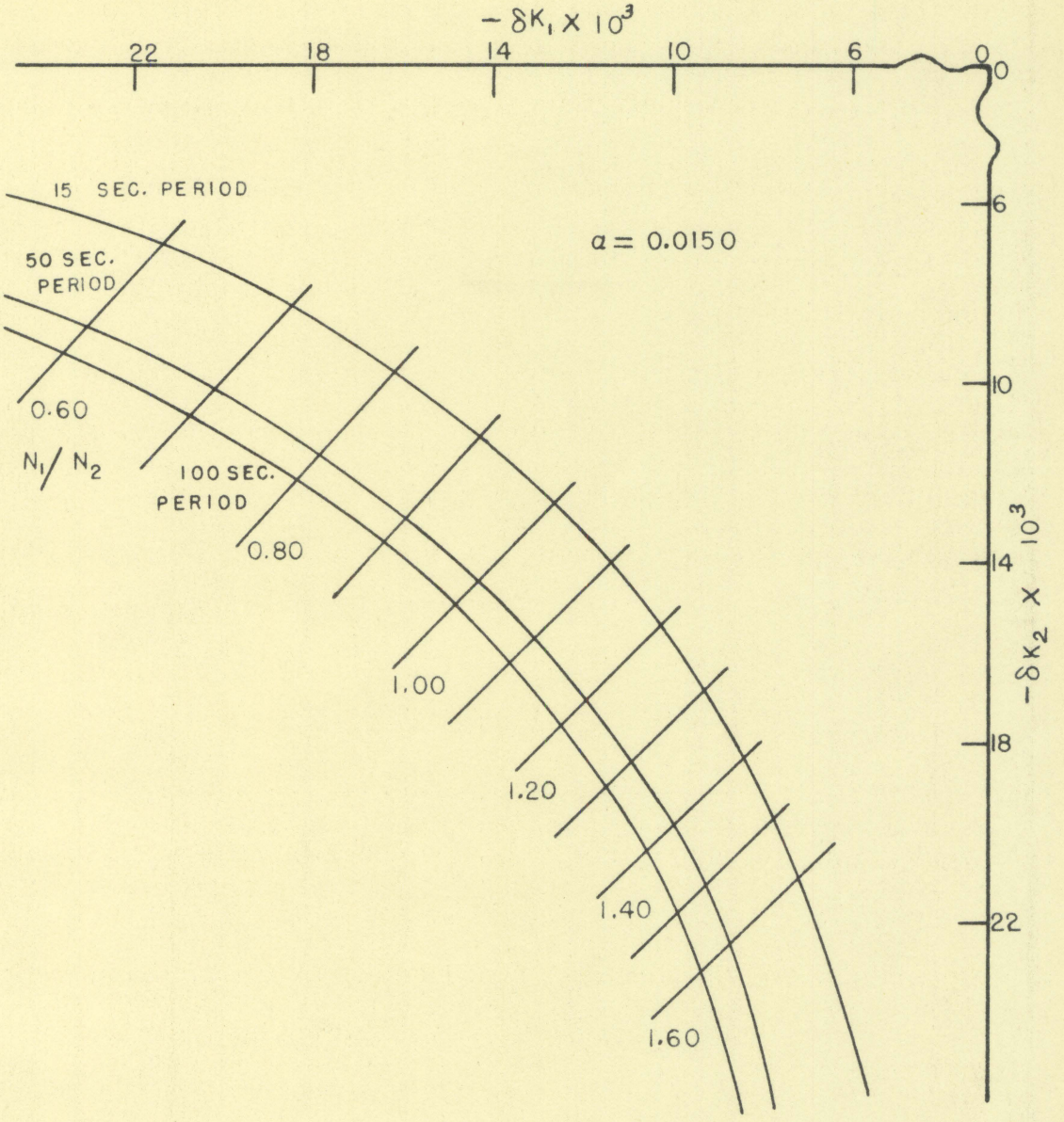

Figure 13. Reactor periods for various values of δK_1 and δK_2

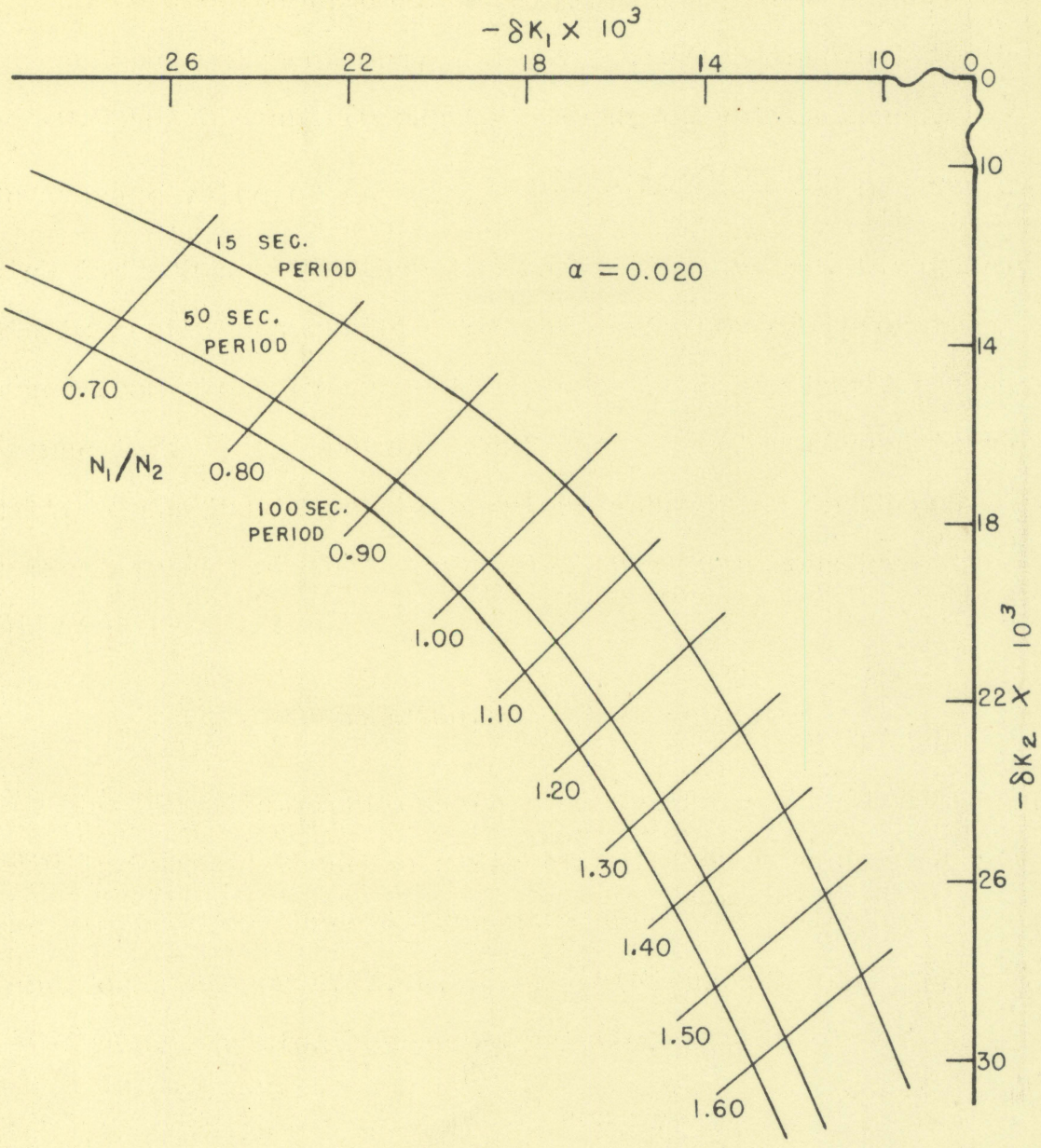

Figure 14. Reactor periods for various values of δK_1 and δK_2

Figure 15. Typical computer results for sinusoidal variations of coupling

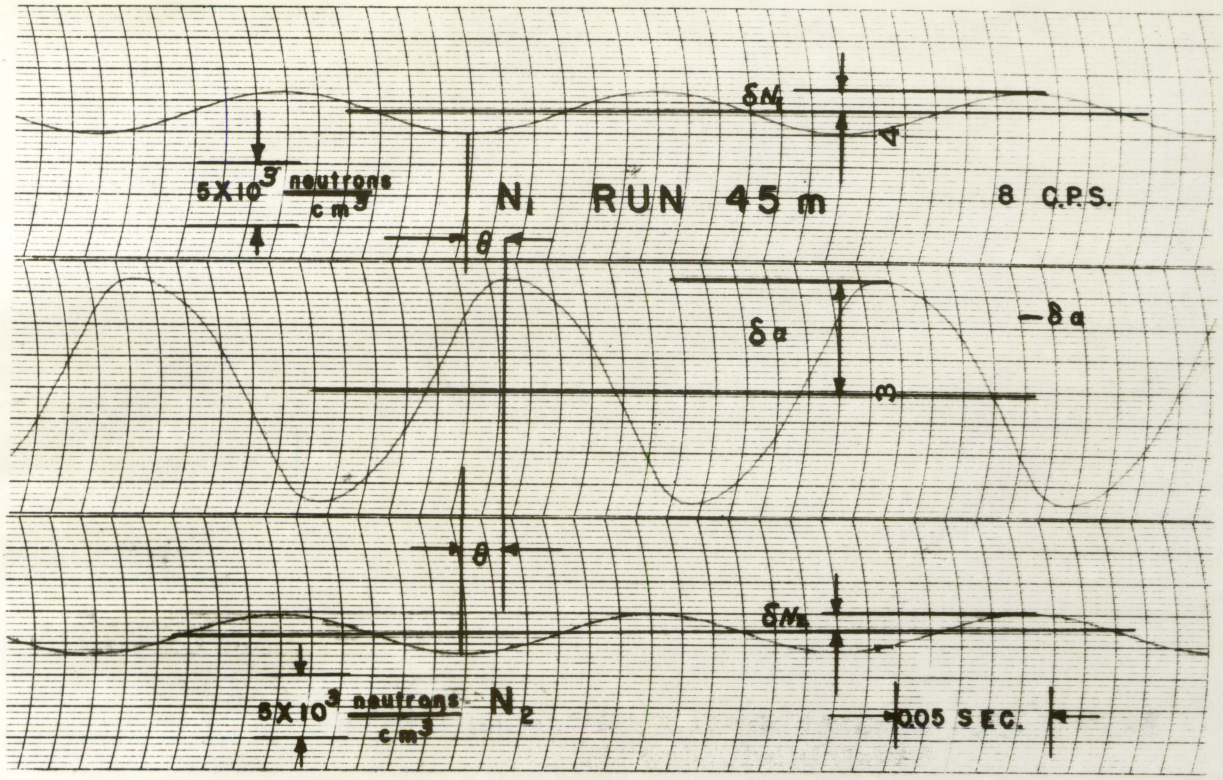
δN1
5X10³ neutrons/cm³
N1 RUN 45 m
8 C.P.S.
θ
δα
-δα
θ
δN2
5X10³ neutrons/cm³
N2
.005 SEC.

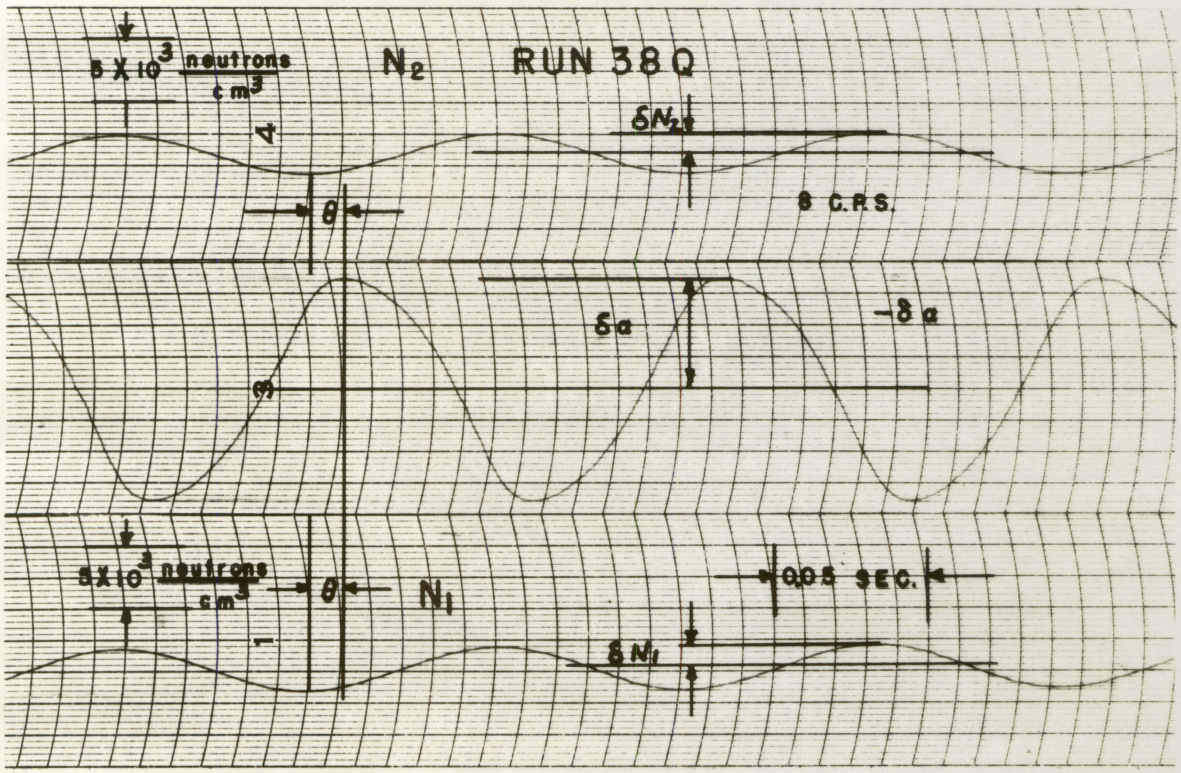
5X10³ neutrons/cm³
N2 RUN 38Q
δN2
8 C.P.S.
θ
δα
-δα
5X10³ neutrons/cm³
θ
N1
.005 SEC.
δN1

the coupling which was put into the computer.

The phase shift between the input α and output δn_1 and δn_2 and the amplitude of the neutron density curve in each slab are shown on the strip chart. The data from these charts were used to make the Bode plots shown in Figures 16, 17, 18 and 19.

A Bode plot shows the relationship between the logarithm of the ratio of the amplitude of the output to the amplitude of the input (called the gain), N_1/α or N_2/α in this case, and the frequency of the driving function. In the case of a linear system the frequency of the output is the same as the input with a phase shift between output and input. This phase shift as a function of frequency is also shown on a Bode plot. The gain is usually plotted in units of decibels, a decibel being defined as

$$db = 20 \log_{10} \frac{\text{output}}{\text{input}} . \qquad (39)$$

In the case of a Bode plot of a reactor transfer function, the decibel gain is usually normalized to the amplitude ratio for 1 cps. This was done in this case; the gain was found from the expression

$$db = 20 \log_{10} \frac{\frac{\text{amp. output}}{\text{amp. input}}}{\left(\frac{\text{amp. output}}{\text{amp. input}}\right) f = 1 \text{ cps}} . \qquad (40)$$

This means that the amplitude curve passes through zero gain at 1 cps. The gain is shown in Figures 16 and 17.

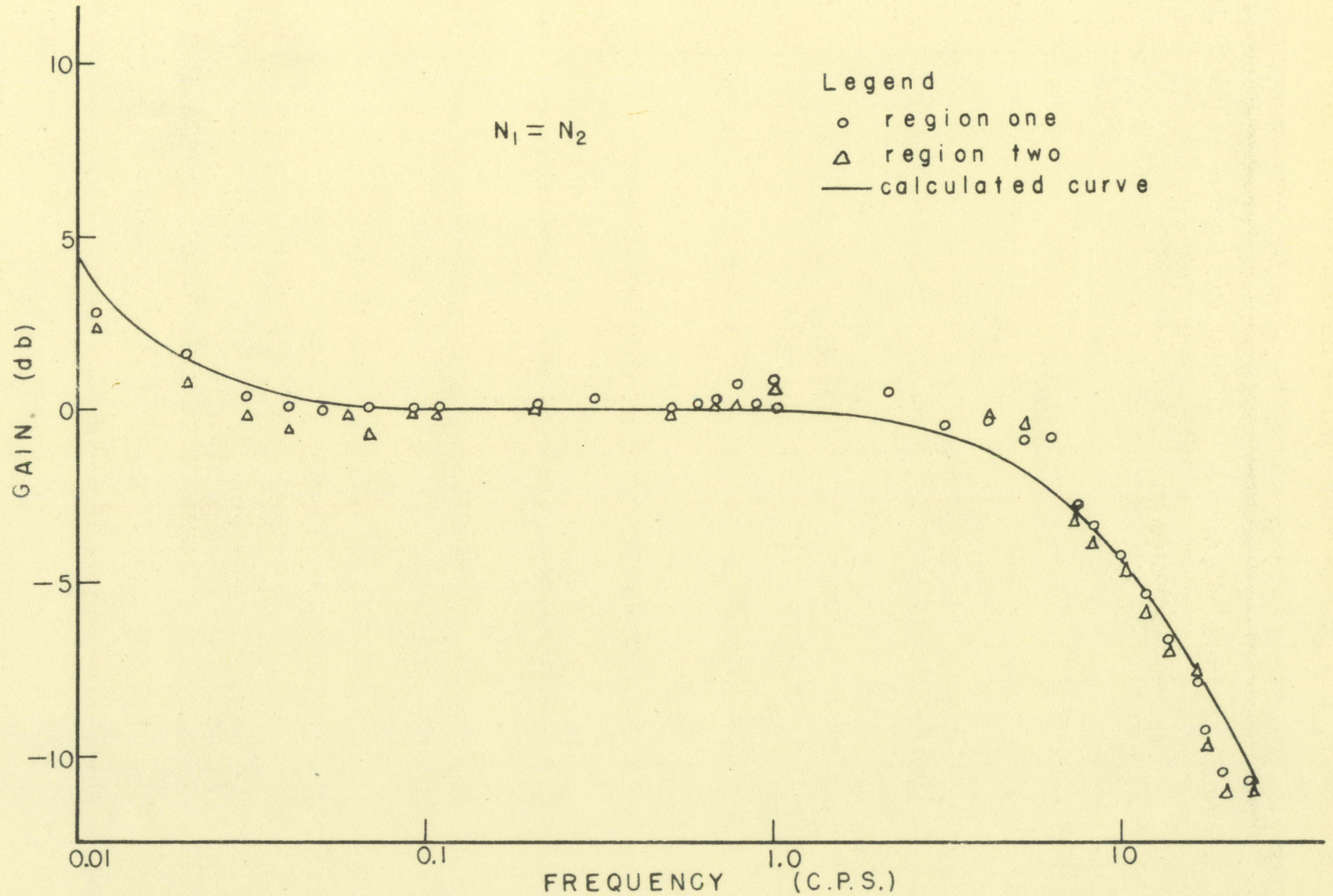

Figure 16. Gain versus frequency for conditions of no flux tilting

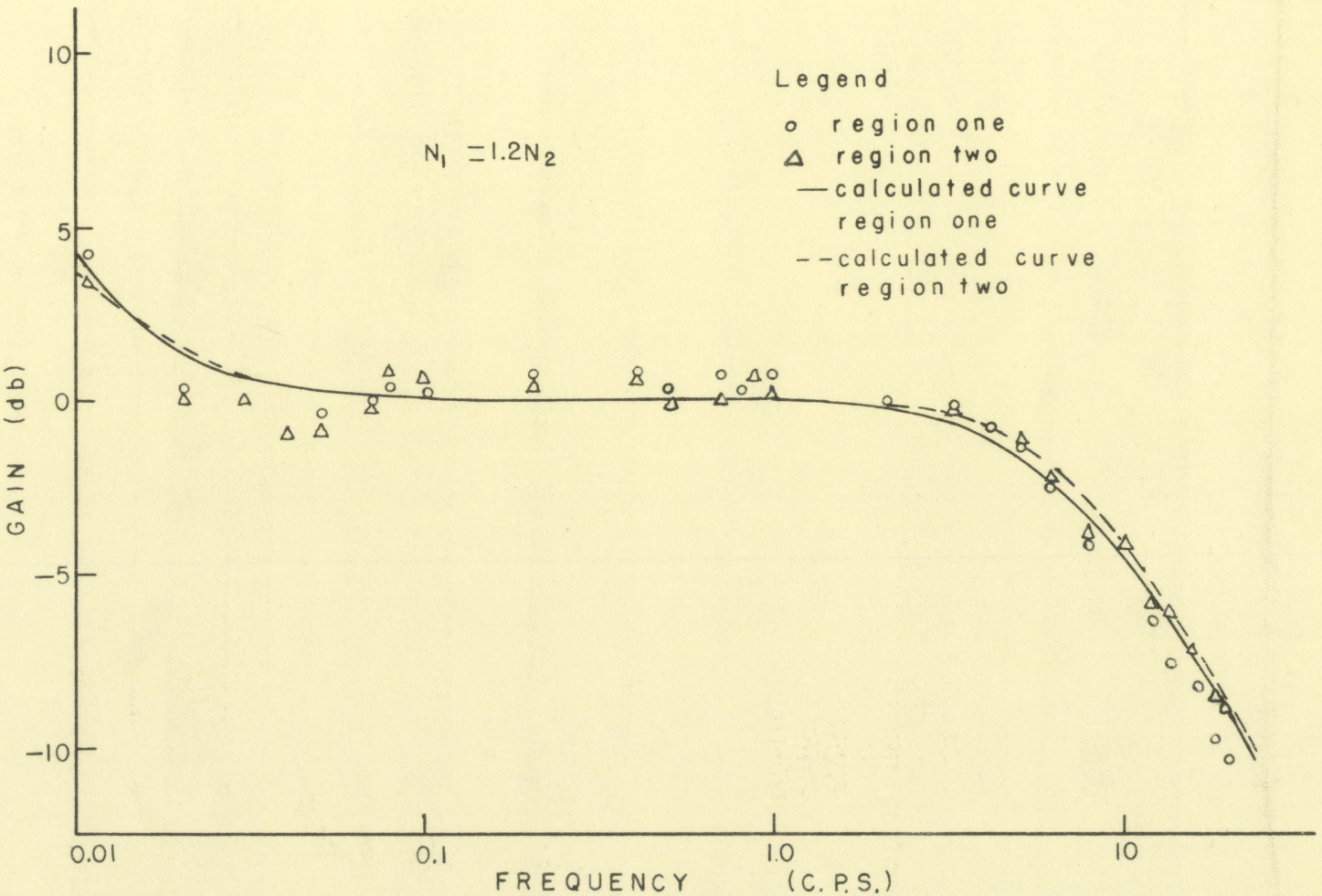

Figure 17. Gain versus frequency with flux tilting present

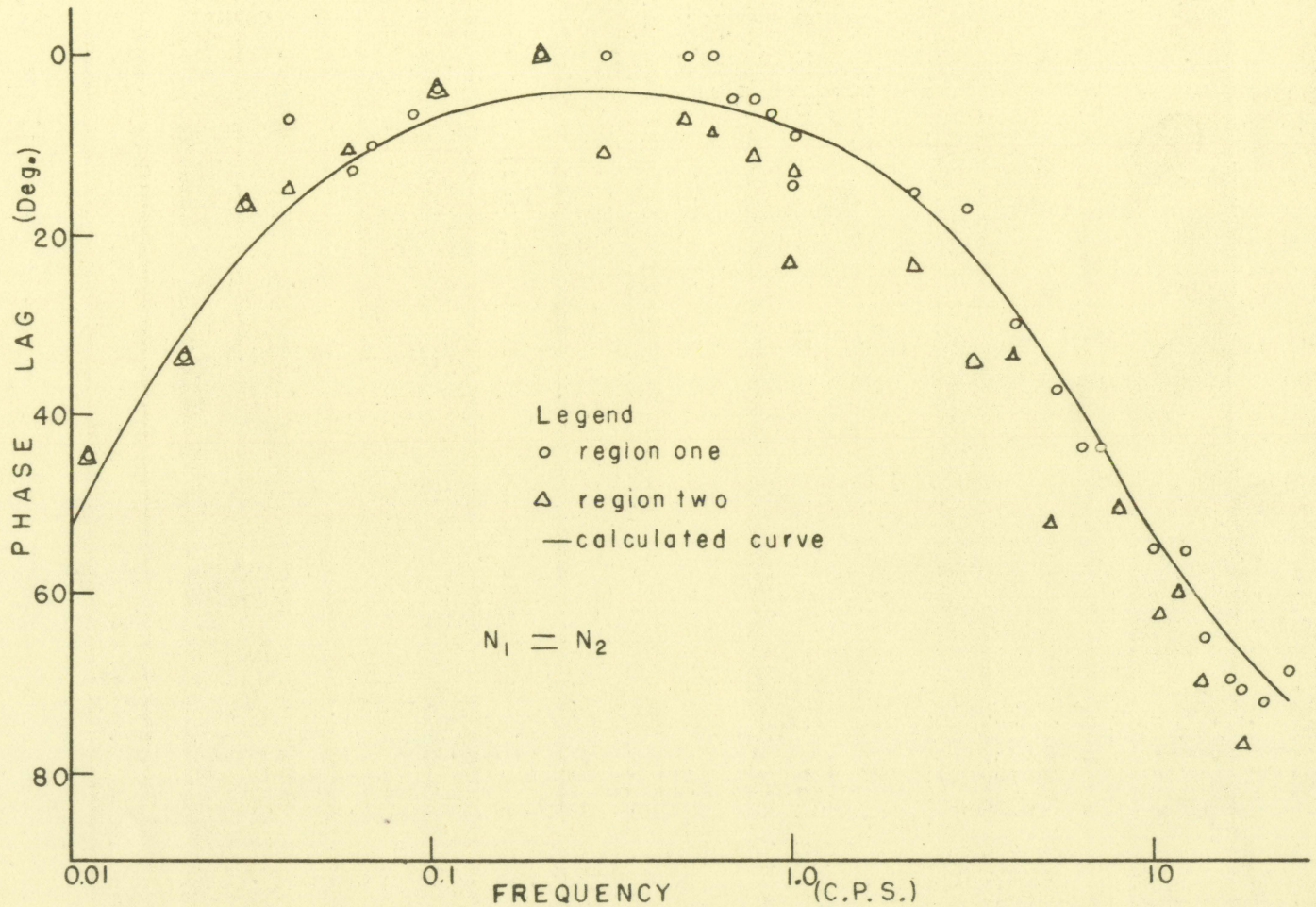

Figure 18. Phase lag versus frequency for conditions of no flux tilting

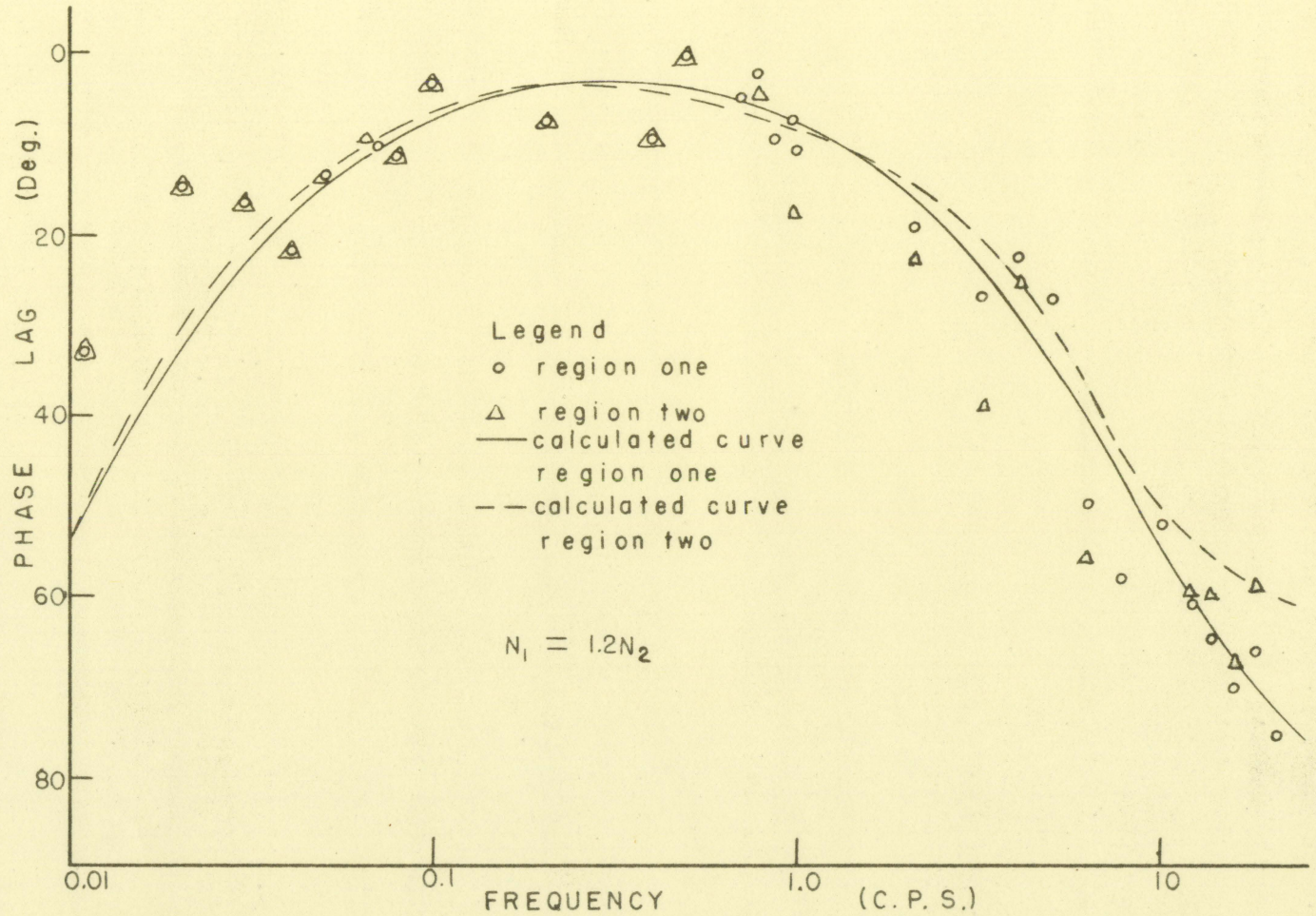

Figure 19. Phase lag versus frequency with flux tilting present

The phase shift is shown in Figures 18 and 19. The phase shift is the angle that the output leads or lags the input. In the cases considered here the output lags the input over the range of frequencies considered. The phase shift, θ, was determined from

$$\theta^{\circ} = \frac{A - B}{C} (360^{\circ}) \qquad (41)$$

where

A = number of chart divisions measured from some common reference to the maximum of neutron density curve

B = number of chart divisions measured from the same common reference to the maximum of the coupling curve

C = number of chart divisions for 360 degrees.

The Bode plots of the reactor transfer functions using Equations 77 and 78 which are derived in Appendix B are also shown on Figures 16, 17, 18 and 19. Equations 77 and 78 were expanded and numerical values were substituted for the symbols. The equation for no flux tilting becomes

$$\frac{\delta n_2(S)}{\delta \alpha(S)} = \frac{\delta n_1(S)}{\delta \alpha(S)} = \frac{n_{10}(S + 0.08)}{S(S + 48.1)} \qquad (42)$$

With n_{10}/n_{20} equal to 1.2 the transfer function for each region is different and the following equations result

$$\frac{\delta n_1(S)}{\delta \alpha(S)} = n_{10} \frac{(S + 324)(S + 0.068)(S + 0.08)}{S(S + 280)(S + 0.0665)(S + 48.1)} \qquad (43)$$

$$\frac{\delta n_2(s)}{\delta \alpha(s)} = n_{20} \frac{(s + 240)(s + 0.0639)(s + 0.08)}{s(s + 280)(s + 0.0665)(s + 48.1)} \qquad (44)$$

For purposes of calculations the Laplace operator S was replaced by $j\omega$. The symbol ω represents the frequency of oscillation of the coupling. Values of ω were assumed and the resulting gain and phase shift were calculated.

For all cases the gain was normalized to the gain at 1 cps.

Ramp Inputs of Reactivity

Typical curves obtained for shim rod withdrawals are shown in Figure 20. Run 1-G illustrates the behavior of the two regions during shim rod withdrawal with no flux tilting present at the beginning of rod movement. Run 4-G shows the behavior with flux tilting present; the initial value of N_1/N_2 being 2.00. The high side is in the region from which the rod is being withdrawn. Run 6-G illustrates the behavior with the flux tilted the other way; the low side in the region from which the rod is being withdrawn. The curve marked δ K is the recorded signal from the follow-up potentiometer of the servo-multiplier which was proportional to the reactivity input to the computer.

The data were taken from the strip charts and replotted in the form shown in Figures 21, 22 and 23. The relative neutron level in each region N/N_o was plotted versus δ K

Figure 20. Typical computer results for ramp input of reactivity

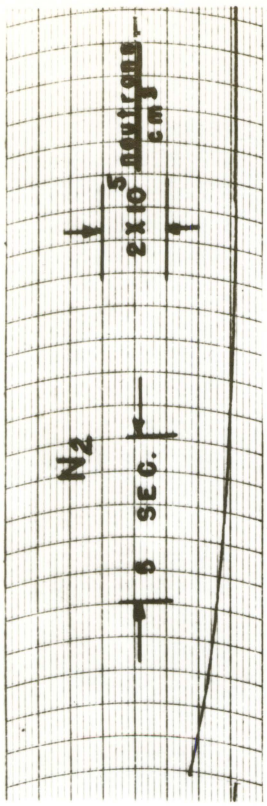
N2
2 x 10^5 neutrons / cm^3
SEC.

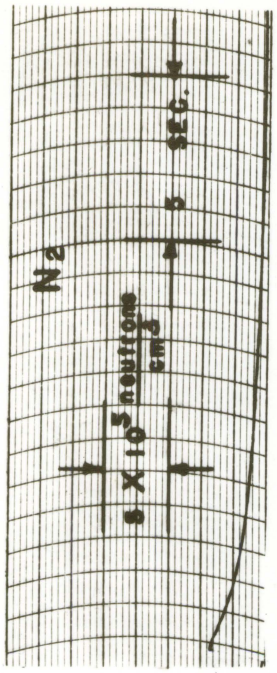
N2
8 x 10^5 neutrons / cm^3
SEC.

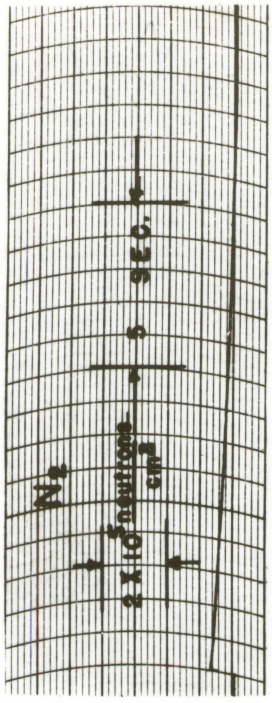
N2
2 x 10^5 neutrons / cm^3
SEC.

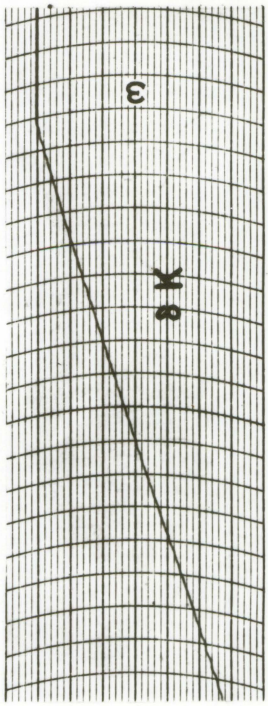
3
8K

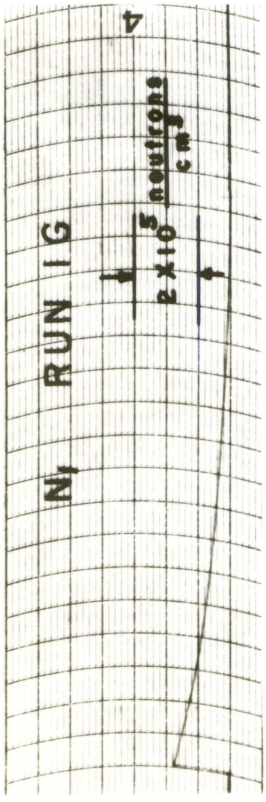
N1 RUN 1 G
4
2 x 10^5 neutrons / cm^3

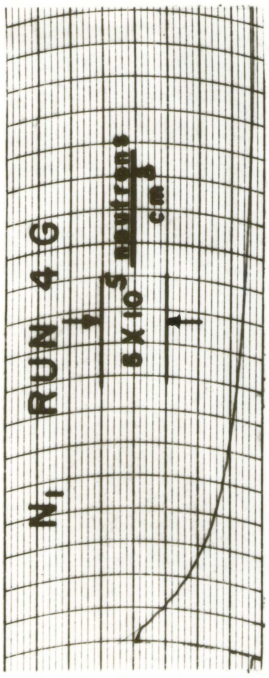
N1 RUN 4 G
8 x 10^5 neutrons / cm^3

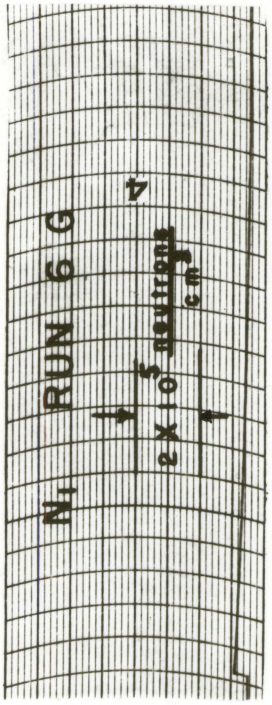
N1 RUN 6 G
4
2 x 10^5 neutrons / cm^3

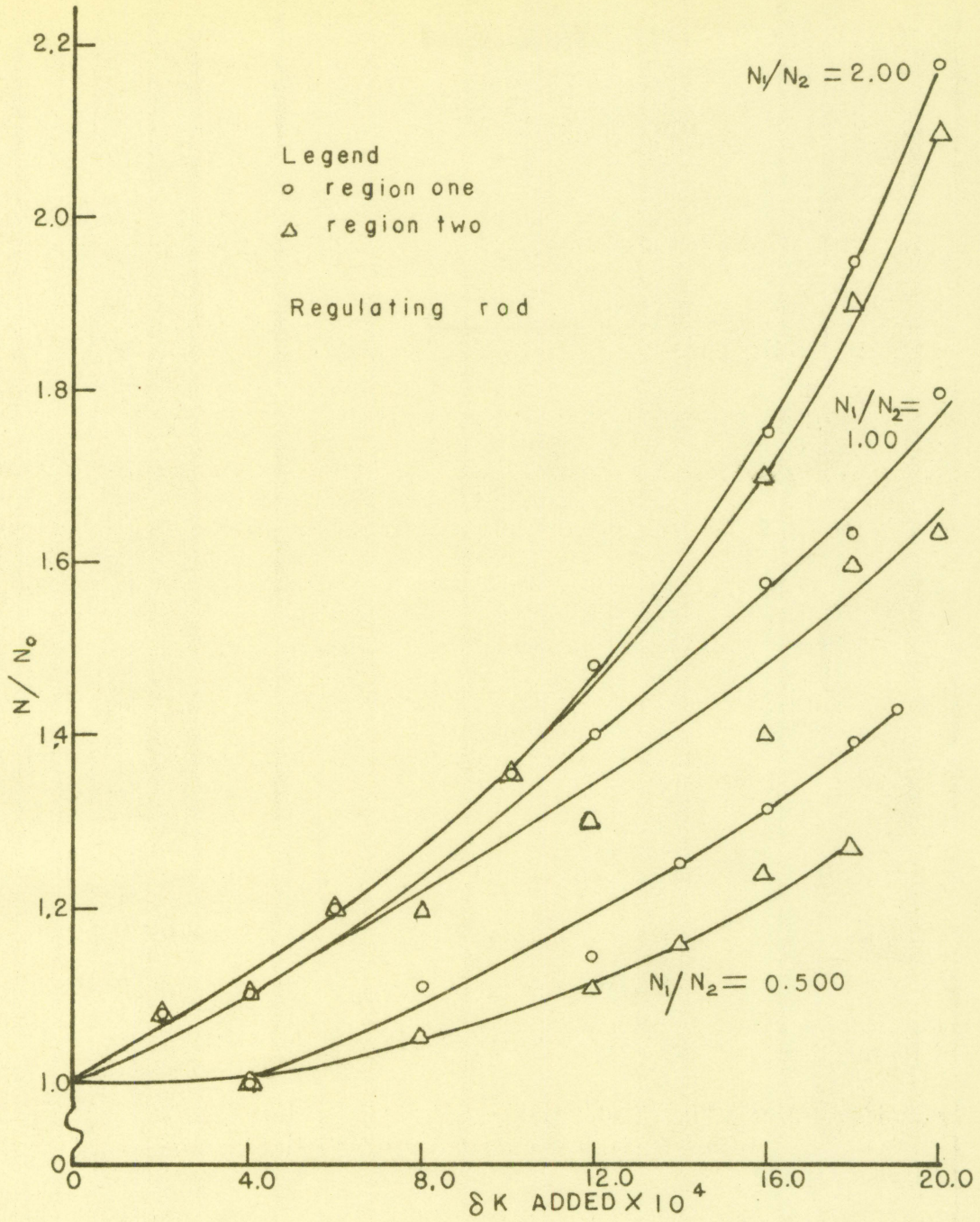

Figure 21. Behavior of reactor for ramp input of reactivity using the regulating rod

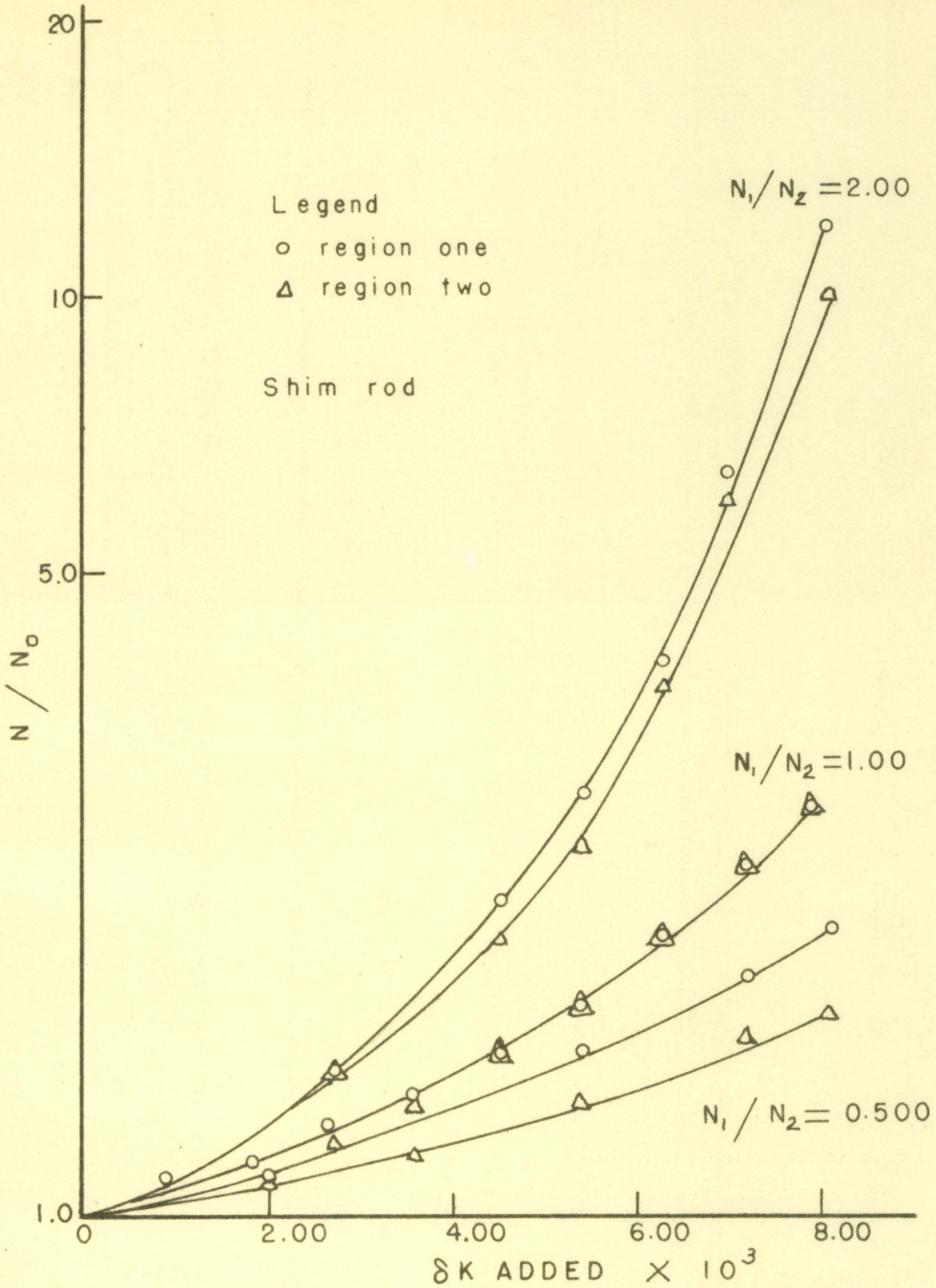

Figure 22. Behavior of reactor for ramp input of reactivity using the shim rod

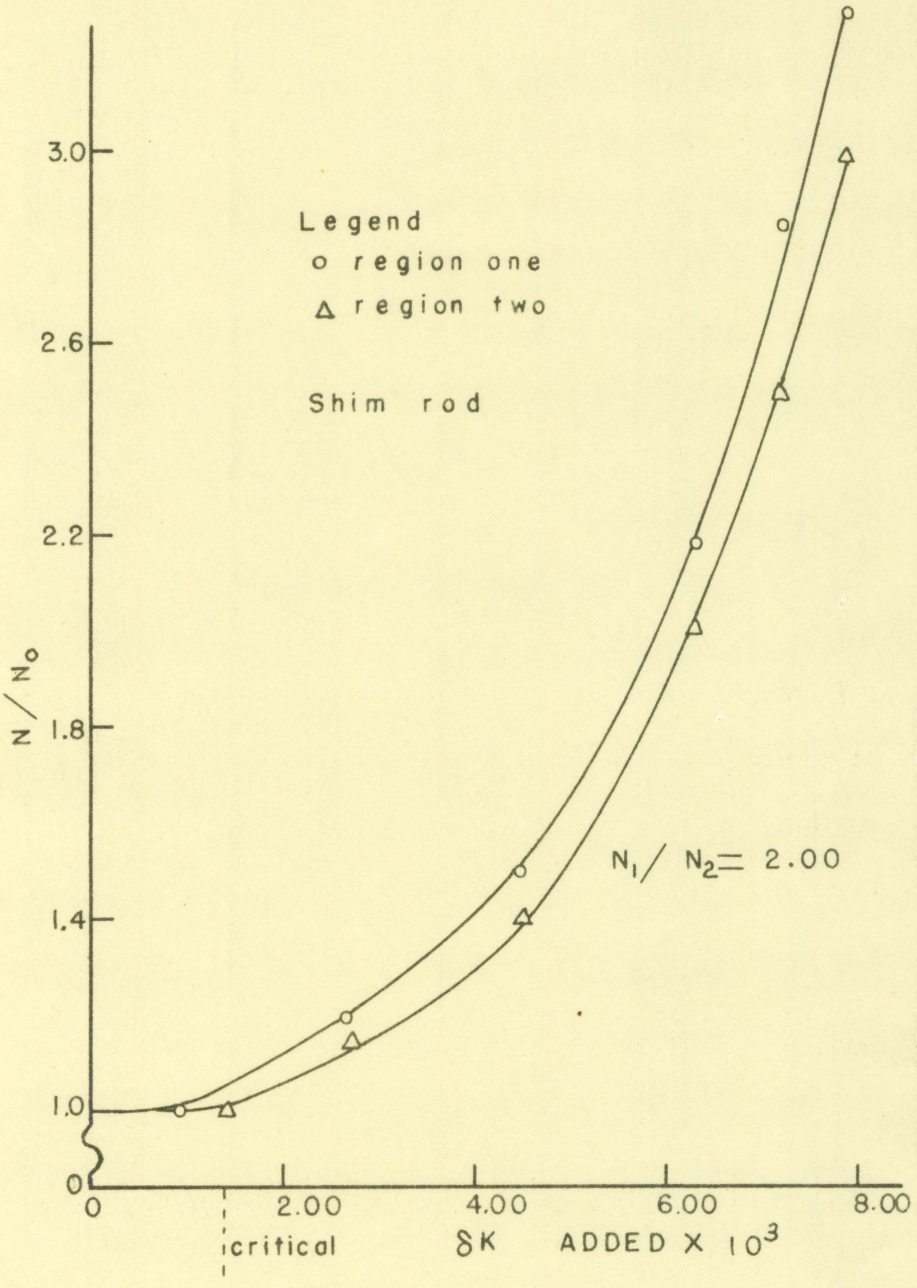

Figure 23. Behavior of reactor for ramp input of reactivity with reactor subcritical

introduced into the reactor. Figure 21 shows the behavior of the two regions during regulating rod withdrawal with various degrees of flux tilting present at the beginning of rod movement. Figure 22 shows the behavior during shim rod withdrawal. All of the curves shown in Figures 21 and 22 present the behavior when the reactor is just critical at the time rod movement is started. (The maximum power level attained during rod withdrawal is greatest for this condition.) Figure 23 illustrates the behavior when rod movement is started when the reactor is subcritical with a source present.

The ratio of N/N_o was obtained from the recorder traces where N_o is the initial neutron density at the time rod withdrawal was started and N is the instantaneous neutron density.

Ramp Input with Sinusoidal Variations of Coupling

Typical results obtained from the computer are shown in Figure 24. The curves of this figure show the reactor behavior during shim rod withdrawal with the oscillator operating. These data were not replotted as it was felt that the effects of the oscillation of coupling on reactor behavior could be observed from these original recorded data.

Figure 24. Typical computer results for ramp input with sinusoidal variation of coupling

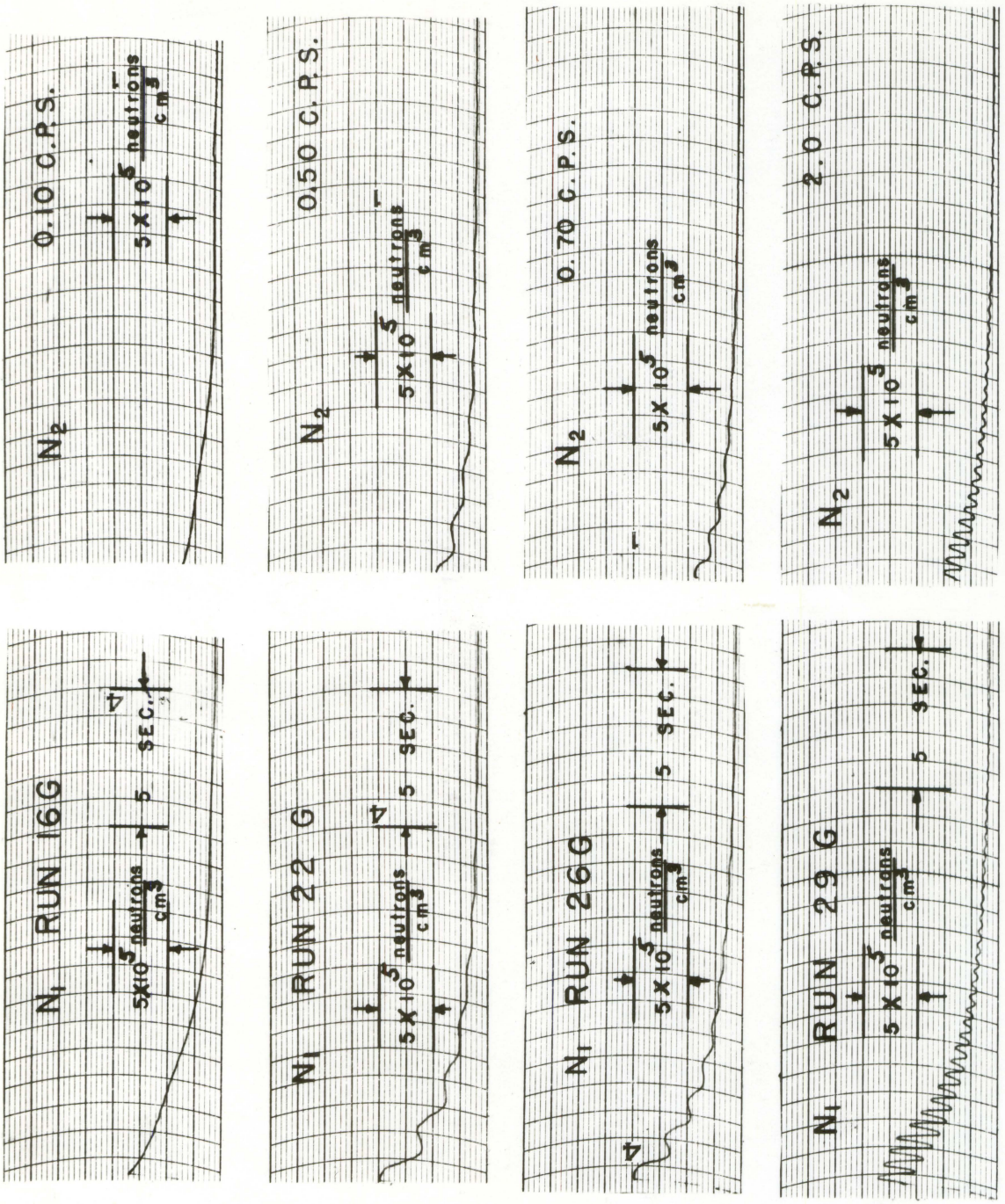
N2
0.10 C.P.S.
5X10^5 neutrons/cm^3
N2
0.50 C.P.S.
5X10^5 neutrons/cm^3
N2
0.70 C.P.S.
5X10^5 neutrons/cm^3
N2
2.0 C.P.S.
5X10^5 neutrons/cm^3
N1 RUN 16G
5X10^5 neutrons/cm^3
5 SEC.
N1 RUN 22 G
5X10^5 neutrons/cm^3
5 SEC.
N1 RUN 26G
5X10^5 neutrons/cm^3
5 SEC.
N1 RUN 29 G
5X10^5 neutrons/cm^3
5 SEC.

DISCUSSION OF RESULTS

The response of the UTR-10 reactor to various types of reactivity disturbances has been studied. The purposes of this section are to interpret the results that have been obtained with the purpose in view of answering the following questions.

1. How do the two core regions of the reactor respond to step inputs of reactivity?
2. What is the effect of changing the coupling interaction between core regions?
3. Is the response of the reactor to a sinusoidal variation in coupling significantly different than the commonly accepted frequency response of a single region reactor?
4. How does flux tilting affect control rod worth?
5. What is the combined effect of coupling oscillation and ramp input of reactivity?

Step Inputs of Reactivity

Typical results obtained from the computer are shown in Figure 7. In run 5D the high side of the tilted flux was in region one, in run 25D the flux was not tilted and run 40D the high side was in region two. Both regions of the reactor exhibit the same stable reactor period and after establishment of this stable period the ratio of N_1/N_2 or ϕ_1/ϕ_2 remains

constant. The ratio of N_1/N_2 or ϕ_1/ϕ_2 can be different than unity, that is under certain conditions flux tilting is possible. This means the power level in one region would be different than in the other. Practically, flux tilting could develop as a result of variations of control rod positions on each side of the reactor. The UTR-10 has one safety rod and the shim rod adjacent to one slab and the other safety rod and the regulating rod next to the other slab. During normal operation the reactor is operated with both safety rods completely withdrawn so therefore the shim and regulating rods are the only rods which can effect individual slab reactivity. For example, suppose the reactor is operating with the regulating rod fully withdrawn and the shim rod partially inserted. This would have the effect of causing the combined multiplication factor for the two regions to be different, resulting in flux tilting. Figure 11 illustrates that extreme flux tilting conditions are possible if the difference between the two slab reactivities is great enough.

The effect of changing the value of the coupling interaction between regions can be seen by comparing Figures 11, 12, 13 and 14. These are typical of those obtained for the range of values of the coupling term that were considered. Decreasing the value of the coupling constant means physically that the two regions are more loosely coupled. Decreasing the degree of coupling between regions causes the flux tilt-

ing behavior to be more sensitive to a given reactivity change than the more closely coupled case, for example compare Figures 11 and 14. This behavior seems reasonable because the larger the value of the coupling the more closely the two regions should behave as a single region, and the more loosely coupled the more independent their behavior. The effect of variations of coupling on reactor behavior is summarized in Figure 25. Data were taken from Figures 11, 12, 13 and 14 to obtain these curves.

The coupling interaction between regions could be varied in several ways; by increasing or decreasing the separation distance between regions, by introducing an absorber into the region between the core tanks or by changing the moderating material between the regions. Since the spacing distance between the core tanks in the UTR-10 is fixed the first method of changing coupling is not possible. A stringer is located in the graphite between the core tanks, so it is possible to introduce an absorber into the region. The effect of the absorber on coupling would have to be determined experimentally, but it would be a function of the neutron absorption cross section and quantity of the material introduced. Since a decrease in coupling between regions results in an overall decrease in the reactivity of the system no safety problem should result. The effect of coupling on reactivity can be seen from Figure 25. The more loosely

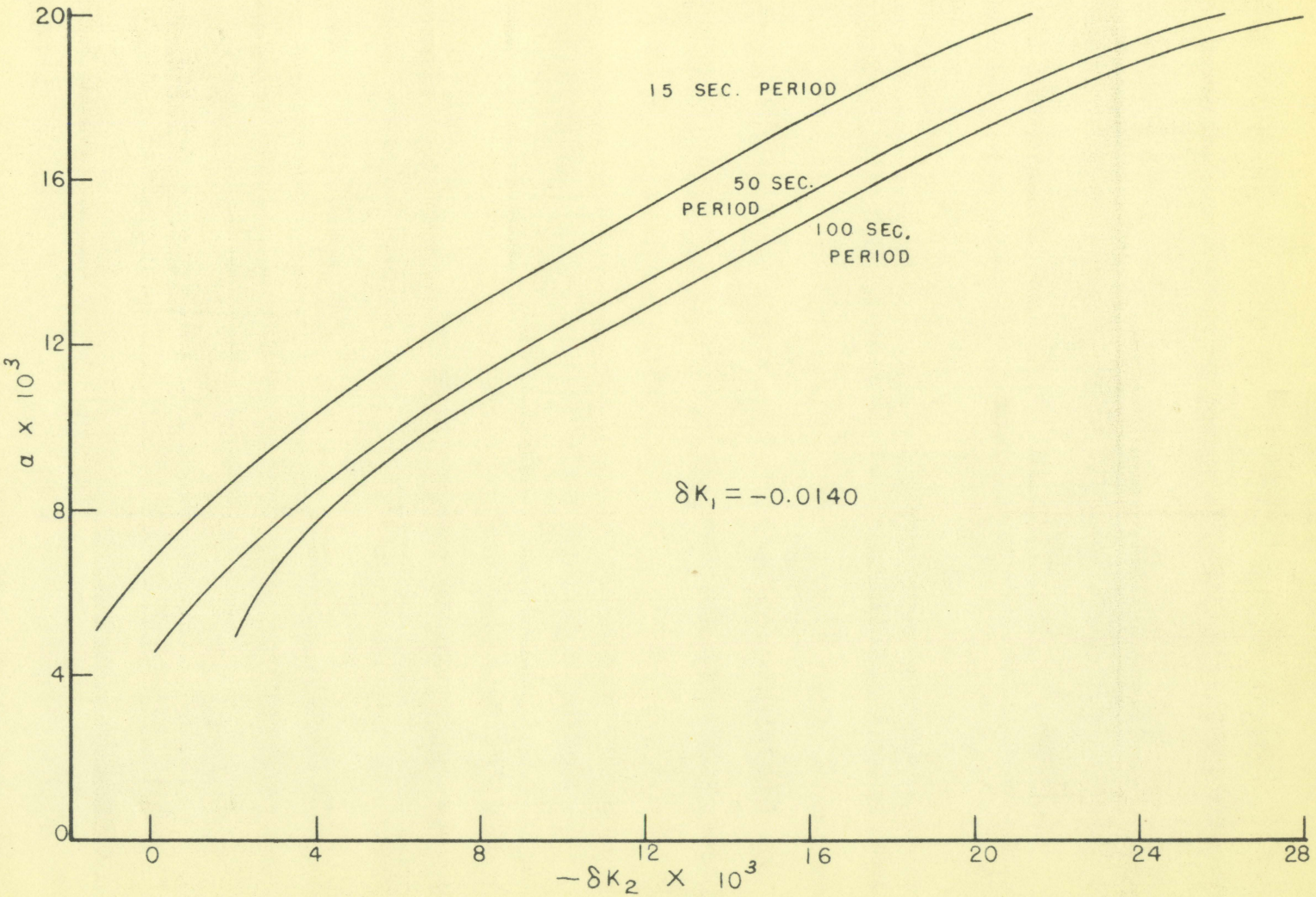

Figure 25. Effect of coupling on reactor period

coupled system requires the larger individual slab reactivity (smaller negative number) for a given reactor period. Therefore, decreasing coupling decreases the overall reactivity of the system as pointed out above. Replacing the graphite with some other moderating material would require structural changes and probably a separate hazards analysis so this change would certainly not be significant during routine reactor operation.

In summary, it has been shown that the two core system exhibits a single stable period, but flux tilting is possible. Changing the value of the coupling interaction affects the flux tilting tendency of the system and the effective reactivity of the overall system.

Sinusoidal Variations of the Coupling Constant

Figures 16, 17, 18 and 19 are Bode plots of the open loop frequency response of the reactor to sinusoidal variations of coupling. The curve of Figure 16 is for the condition of no flux tilting during oscillator operation and Figure 17 presents the response with flux tilting present, N_1 equal to 1.2 N_2. The general shape of the gain curves is similar to that normally obtained for the open loop response of a single region reactor driven by a sinusoidal variation in reactivity, for example see Schultz (29, p. 45).

Operation of the oscillator with flux tilting present

results in slightly different frequency responses in the two slabs. The gain of each region is identical over the frequency range from approximately 0.04 cps to 1.00 cps. Below 0.04 cps and above 1.00 cps the gain of each region is slightly different. This difference in gain is less than one decibel over the range of frequencies considered.

The phase shift curves of Figures 18 and 19 with the flux tilted and with no flux tilting present are similar. The phase shift is slightly different in the two regions when the flux is tilted. The difference is not more than three degrees over the frequency range from 0.01 to 8.00 cps. Above this range a larger difference results, however the theoretical equations indicate that the phase shift for both regions approaches -90 degrees at high frequencies and also at low frequencies. These curves are similar to that obtained for a single region reactor. The output (neutron density) lags the input (coupling) and in all cases the lag angle is less than 90 degrees.

It was found that results obtained when other values of the steady state coupling and other amplitudes of oscillation were used were not significantly different than the results shown.

The open loop frequency response, with or without flux tilting, of the two slab reactor has been shown to be similar to that normally obtained for a single region reactor. The

phase shift and gain are essentially the same as that obtained for the usual case. No unusual behavior which would present a safety problem seems likely.

Good agreement between computer results and the theoretical transfer functions, Equations 42, 43 and 44, were obtained.

Ramp Inputs of Reactivity

The effect of flux tilting on control rod effectiveness can be observed by considering Figures 20, 21, 22 and 23. Figure 20 presents results which are typical of those obtained from the computer. Figure 21 illustrates the behavior during regulation rod withdrawal. The rod was removed from the region in which the neutron density is designated as N_1. The curves shown illustrate the behavior under three conditions; flux initially tilted with the high side in the region from which the rod is being withdrawn, no flux tilting initially present at beginning of rod movement, and the flux initially tilted with the low side in the region from which the rod is being withdrawn. Figure 22 presents similar conditions for shim rod withdrawal. In both cases rod movement was started with the reactor just critical. Figure 23 illustrates the behavior during shim rod withdrawal with the reactor subcritical with a source present at the time of rod movement was started. The condition resulting in the most rapid increase in power level is with the flux initially

tilted with the high side in the region from which the rod is being withdrawn.

It is evident from these results that flux tilting can affect the apparent worth of the rod. For example, in Figure 22, it can be seen that if shim rod withdrawal is started when the neutron flux is tilted with the high side in the region from which the rod is being withdrawn, an increase of power of approximately ten is obtained, whereas if the flux is tilted the other way an increase of about two is obtained. In most cases the power level of the region opposite the one from which the rod is being removed lags. This is to be expected since the rod being moved affects the reactivity of the adjacent region, and it is only through the coupling interaction that the reactivity of the opposite region is increased.

As discussed by Baldwin (4) flux tilting can affect control rod calibration; the use of the normal inhour equation for a two core system can result in erroneous rod worth data. This is illustrated by the discussion which follows. The usual procedure used in rod calibration consist of maintaining the reactor at a constant power level and then withdrawing a rod a given amount. The resulting reactor period is then determined and related to the reactivity worth of the portion of the rod moved by using the inhour equation. Figure 26 presents a plot of reactor period versus reactivity.

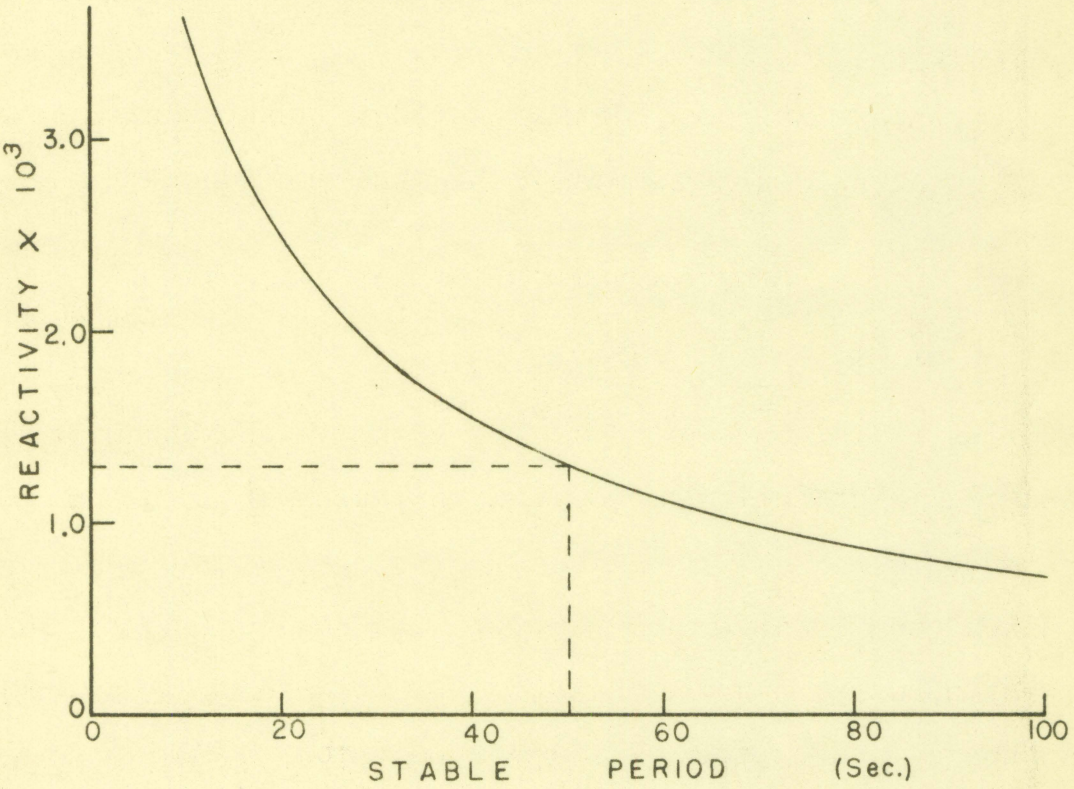

Figure 26. Reactivity versus reactor period

This curve was obtained from the inhour equation using UTR-10 data:

$$\frac{\delta K}{K} = \frac{\ell}{\tau K_{eff}} + \frac{\beta}{1 + \lambda\tau} \qquad (45)$$

where

$\frac{\delta K}{K}$ = reactivity, $K_{eff}-1/K_{eff}$

ℓ = neutron lifetime, sec

τ = reactor period, sec^{-1}

K_{eff} = effective multiplication factor

β = delayed neutron fraction

λ = decay constant for delayed neutron precursors, sec^{-1}

Suppose for purposes of illustration that a rod is removed from the reactor resulting in a 50 second period. Using the inhour curve of Figure 26 the apparent reactivity worth of the length of rod moved is 0.00130. This value can be compared with the worth predicted by considering the two core system. The assumption is made that δK and reactivity are equal for the following discussion. Suppose that rod movement was started with no flux tilting present; it can then be seen from Figure 27 that the predicted rod worth for a 50 second period is 0.00240 (point A). If rod movement is started with flux tilting present, say N_1/N_2 equal to 0.600, the predicted rod worth is 0.00380 (point B). With the flux tilted the other way with N_1/N_2 equal to 1.40 the predicted worth is 0.00180 (point C). These cases serve to indicate that period alone is not sufficient to establish rod worth in the two

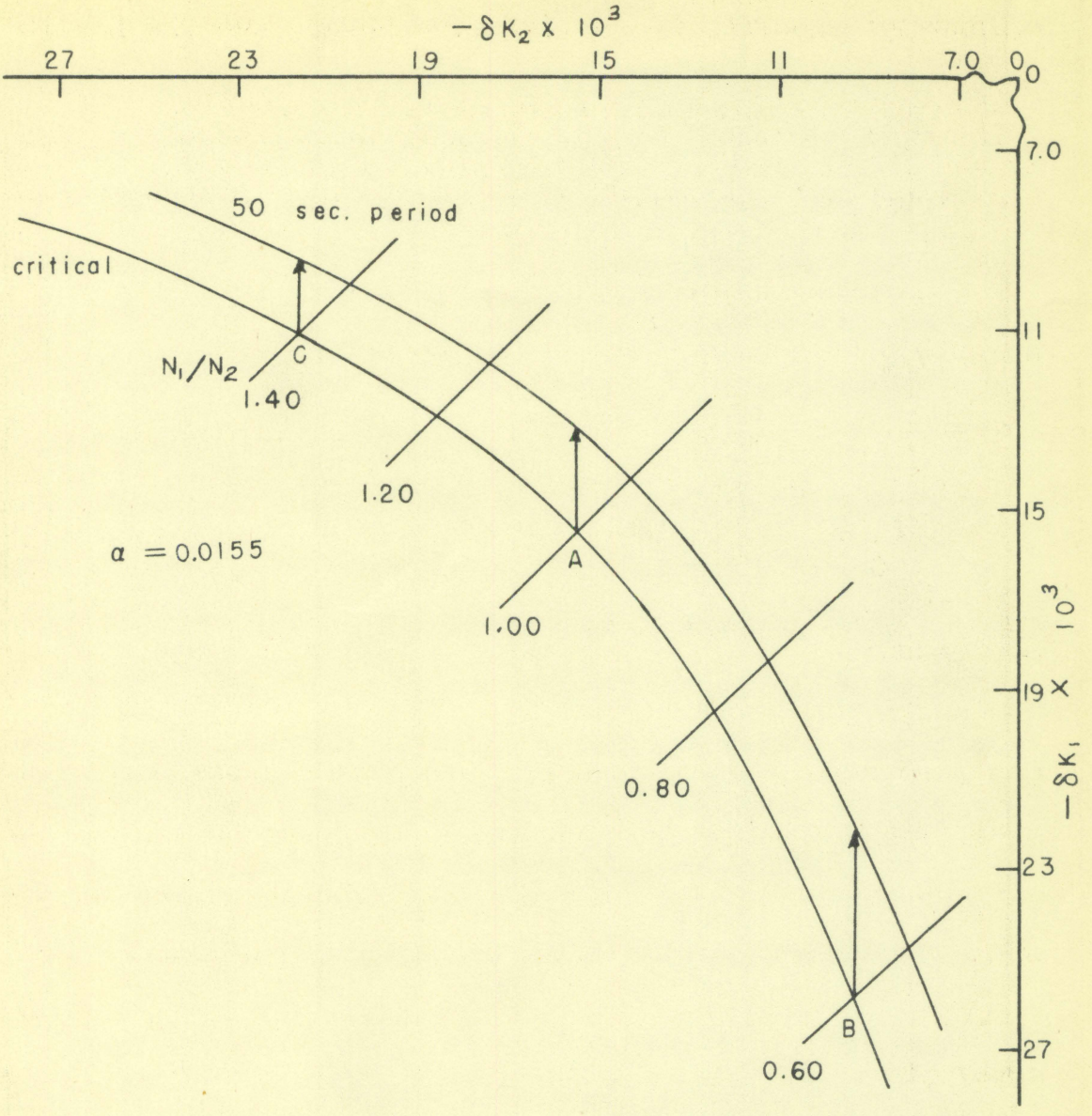

Figure 27. Variation of control rod worth for the two core system

core system. Due to flux tilting the actual rod worth can be quite different than that predicted by the inhour equation. Even with no flux tilting initially present the rod worth as predicted by the inhour equation is in error. If the ratio of neutron fluxes in the two regions is known, one can use a curve similar to that of Figure 27 to determine rod worths. Figure 27 can be thought of as an equivalent inhour curve for the two region system and Equation 52 in Appendix A as an equivalent inhour equation.

In summary, flux tilting has a strong effect on rod worth. The effect of a control rod is much greater if removed from the high flux region than if removed from the low flux region. Rod calibration data can be in error if the normal inhour equation is used to relate reactor period and reactivity. In other words, the effect of flux tilting must be taken into account when considering rod worth.

Ramp Input with Sinusoidal Variations of Coupling

Typical results of this phase of the study are shown in Figure 24. The effect of oscillator operation during rod movement may be observed by comparing the results shown in these figures with run 4G of Figure 20. Only data obtained during shim rod movements are shown since these data were the most significant of all of the conditions studied.

For purposes of illustration consider run 4G of Figure 20 which is for ramp input only, and compare this with runs 16G, 22G, 26G and 29G of Figure 24. It is apparent that no significant power oscillations result until a frequency of 0.50 cps is reached. It is also noted that the amplitude of oscillation increases with increasing power level. This would be expected since the gain of a reactor transfer function is proportional to the steady state neutron level.

The effect of flux tilting on power level reached during rod withdrawal is comparable to the behavior without the oscillator running. The worth of a rod located in the high flux region is greater than the rod located in the low flux side. Flux tilting results in different amplitudes of oscillation in the two regions.

In summary, it has been shown that oscillator operation during control rod movement results in power oscillation of increasing amplitude with increasing power level. Flux tilting results in an increase of the amplitude of the power surges. It is felt that these results indicate that it would be good operating procedure to use the oscillator only when the reactor is operating at a constant power level.

Degree of Flux Tilting in the UTR-10

The effects of flux tilting on control rod worth and on reactor behavior have been discussed. The conclusions reached

are valid if no limitations are placed on how control rods are positioned or on the excess reactivity placed in the core. The purpose of this section is to discuss how the actual rod worths and reactivity in the core limit the amount of flux tilting that can be developed. An attempt is made to answer the question, how significant is flux tilting in the UTR-10?

Figure 28 presents rod calibration curves obtained at the time of initial reactor startup for the shim and regulating rods of the UTR-10. As pointed out previously, the safety rods are completely withdrawn from the core during operation so therefore their affect on flux tilting will not be considered. The rod calibration curves shown were determined by the usual method of relating reactor period to excess reactivity through the inhour equation. It is assumed for this discussion that the effects of flux tilting on these rod curves is a second order effect so therefore these rod worths are assumed to be correct for any value of flux tilting.

The excess reactivity of the reactor was established as 0.49 per cent at the time of initial startup. Referring to Figure 29 it can be seen that for just critical conditions and for a flux ratio of unity,

$$(\delta K_1) = (\delta K)_2 = -0.0155 .$$

Each region is subcritical by this amount. It is assumed that δK and reactivity can be used interchangeably in this

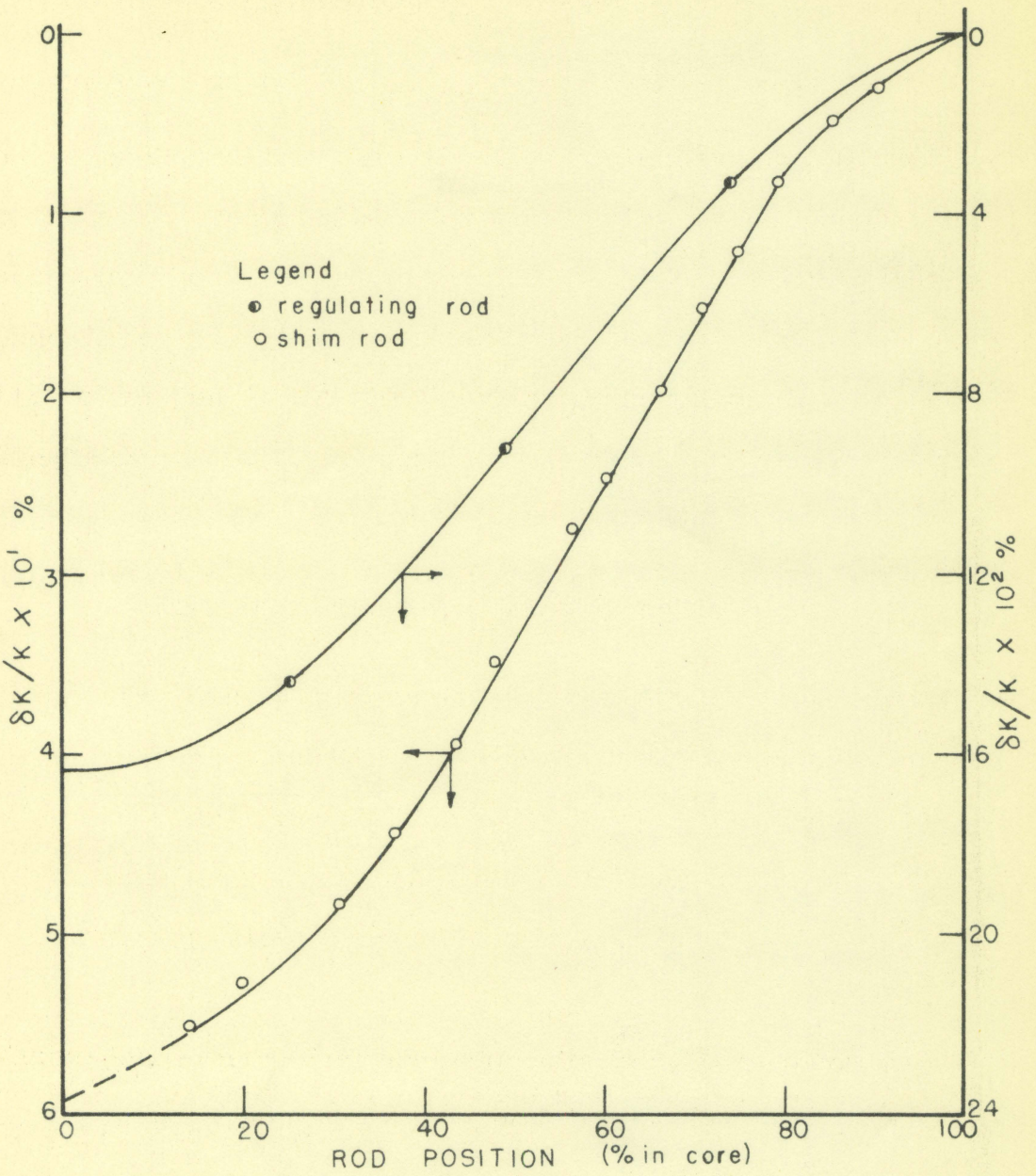

Figure 28. Control rod calibration curves for the UTR-10 reactor

discussion. If it is assumed that the excess reactivity, 0.49 per cent, is divided equally between the two regions, the excess reactivity of each region is

$$(\delta K)_1 = (\delta K)_2 = - 0.0155 + 0.00245$$
$$= - 0.0131 .$$

The two extreme operating conditions possible are; the regulation rod completely inserted in the core or the regulation rod completely withdrawn. It is assumed that the regulating rod is adjacent to region one and the shim rod is adjacent to region two. Consider first the case with the regulating rod completely inserted. The total regulating rod worth from Figure 28 is 0.00164 so therefore region one would have an excess reactivity of

$$(\delta K)_1 = - 0.0131 - 0.00164$$
$$= - 0.0147.$$

This value is located on Figure 29 on the $(\delta K)_1$ axis. The required reactivity of region two is, reading from the curve, -0.0164. Therefore the shim rod must be inserted until the worth of the rod put in is

$$(\delta K)_2 = - 0.0164 - (-0.0131)$$
$$= - 0.00330 .$$

Referring to Figure 28 it can be seen that about 58 per cent of this rod would be in the core. The total negative re-

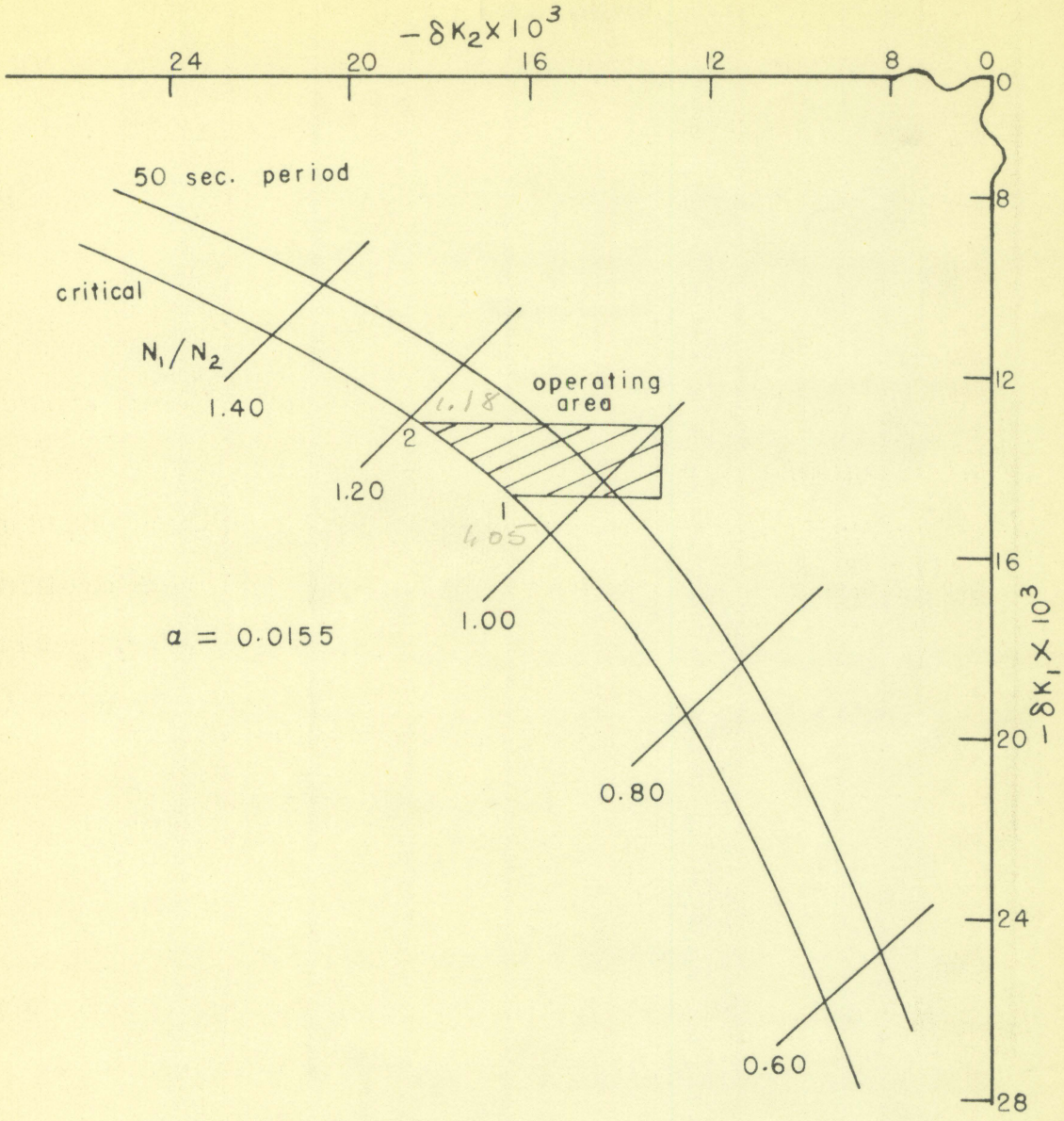

Figure 29. Operating area for the UTR-10 reactor

activity added to the core is

$$0.00330 + 0.00164$$
$$= 0.00490 .$$

just the amount required to handle the excess reactivity of the core. These two reactivity values (-0.0164 and -0.0147) locate point 1 on Figure 29.

Consider the second case with the regulating rod completely withdrawn. The excess reactivity or region one is

$$(\delta K)_1 = - 0.0131.$$

and this value is located on the $(\delta K)_1$ axis of Figure 29. The required reactivity for region two for critical conditions is -0.0180 which means the shim rod would be inserted to add

$$-0.0183 - (-0.0131)$$
$$= - 0.0052.$$

This means the shim rod would be about 76 per cent in the core. These two values of reactivity locate point 2 on Figure 29. Points 1 and 2 represent the extreme flux tilting conditions possible. The possible operating conditions are shown in the blocked in area on Figure 29.

As can be seen in Figure 29 the limited range of control rod worths fixes the amount of flux tilting that can be developed. The methods used in predicting this operating area are only approximate, but it is felt that this procedure

can be used to arrive at a reasonable range of operating conditions of the reactor.

Referring to Figure 29 it can be seen that the maximum degree of flux tilting possible is less than 20 per cent. The high side of the flux profile occurs in the region adjacent to the regulating rod in all critical cases. It is therefore not possible to pull the shim rod with the flux initially tilted with the high side in region two. It will be recalled that this procedure resulted in the worst condition. For this reason it is possible to rule out any unusual behavior during shim rod movement and since the worth of the regulating rod is quite low (less than 0.2 per cent) no significant flux tilting effects should be observed.

CONCLUSIONS

Within the scope of this investigation the following conclusions seem justifiable:

1. Flux tilting across the reactor is possible, however both core regions exhibit the same stable reactor period.
2. A decrease of the coupling interaction between regions decreases the overall reactivity of the system.
3. The response of the reactor to a sinusoidal variation of coupling, with or without flux tilting, is not significantly different than the response of a single region reactor to a sinusoidal variation of reactivity.
4. Flux tilting can affect the worth of a control rod. The apparent worth can be much greater if the rod is removed from the high flux region rather than the low flux region.
5. Rod worth as predicted using the inhour equation can be in error because of the non-separability of the time and space variables. Period alone is not sufficient for predicting rod worth.
6. A flux ratio of unity with the reactor critical is never attained during normal operation. The ratio of ϕ_1/ϕ_2 or N_1/N_2 varies from approximately 1.05 to 1.18 for critical conditions. Because of this

limited range, flux tilting effects should not be significant. If operation with the safety rods partially inserted (not possible in the UTR-10) is attempted, flux tilting could become more significant than it is under the present operating procedure.

7. The reactivity oscillator should be operated only when the reactor is stabilized at a constant power level. Operation during power level changes results in power surges of increasing amplitude with increasing power level.

SUGGESTED TOPICS FOR FUTURE WORK

Several items that would be of interest for future investigation have resulted from this work. The most obvious are:

1. Repeat some of this work, particularly the frequency response portion, using more than one group of delayed neutrons.
2. Attempt to determine the degree of flux tilting experimentally.
3. Experimentally verify the frequency responses curves reported here.

LITERATURE CITED

1. Akcasu, Ziya. General solution of the reactor kinetics equations without feedback. Nuclear Science and Engineering. 3: 456-467. 1958.

2. American Standard Company. Atomic Energy Division. Hazards analysis UTR-10 standard model. Mountain View, California, Author. [ca. 1958].

3. Analog computer use in the nuclear field. Nucleonics 15, No. 5: 88. May, 1957.

4. Baldwin, G. C. Kinetics of a reactor composed of two loosely coupled cores. Nuclear Science and Engineering. 6: 320-327. 1959.

5. _____, Carey, Walter E.; Cilesiz, Ayhan; Kimel, William R.; Klaiber, G. Stanley; Pawlicki, Gerald S.; and Prohammer, Fredric G. Pegagogical applications of an Argonaut reactor. U. S. Atomic Energy Commission Report ANL 5989 [Argonne National Laboratory, Lemont, Illinois]. [ca. 1961].

6. Borner, E. F. and Cassidy, B. F. Analog study of boiler reactor interactions. Nucleonics 15, No. 5: 84-88. May, 1957.

7. Braffort, Paul. The dynamic problems of power reactors and analog computers. [1st.] International Conference on the Peaceful Uses of Atomic Energy, Geneva, 1955. Proc. 5: 369-376. 1956.

8. Chestnut, Harold and Mayer, Robert W. Servomechanisms and regulating system design. Vol. 1. New York, N. Y. John Wiley and Sons, Inc. 1951.

9. Cox, R. J. An introduction to control of nuclear reactors. Nuclear Power 1: 114-117. 1956.

10. _____. An introduction to the control of nuclear reactors. Nuclear Power 1: 161-164. 1956.

11. Franz, Joseph P. Pile transfer functions. U. S. Atomic Energy Commission Report AECD-3260 [Technical Information Service]. 1949.

12. _____ and Alliston, W. H. PWR training simulator. Nucleonics 15, No. 5: 80-83. May, 1957.

13. Glasstone, Samuel and Edlund, Milton C. The elements of nuclear reactor theory. New York, N. Y. D. Van Nostrand Co., Inc. 1952.

14. Griffin, C. W. and Lundholm, J. G. Measurement of the SRE and KEWB prompt neutron lifetime using random noise and reactor oscillator techniques. U. S. Atomic Energy Commission Report NAA-SR-3765 [North American Aviation, Inc. Downey, California]. 1959.

15. Harrer, J. M.; Boyer, R. E.; and Kuucoff, Darwin. Transfer function of Argonne CP-Z reactor. Nucleonics 10, No. 8: 32-36. Aug., 1952.

16. Henry, A. F. and Curlee, N. J. Verification of a method for treating neutron space time problems. Nuclear Science and Engineering. 4: 727-744. 1958.

17. Hurwitz, Henry Jr. Derivation and integration of the pile kinetic equations. Nucleonics 5, [No. 7]: 61-67. July, 1949.

18. Introduction to analog computers. Nucleonics 15, No. 5: 70-71. May, 1957.

19. Isbin, H. S. and Gorman, J. W. Applications of pile-kinetic equations. Nucleonics 10, No. 11: 68-71. Nov., 1958.

20. Johnson, S. O. and Grace, J. N. Analog computation in nuclear engineering. Nucleonics 15, No. 5: 72-75. May, 1957.

21. Keppin, G. R. and Wimett, T. F. Reactor kinetic functions: a new evaluation. Nucleonics 16, No. 10: 86-90. Oct., 1958.

22. Korn, Gravino A. and Korn, Theresa M. Electronic analog computers. 2nd ed. New York, N. Y. McGraw-Hill Book Co., Inc. 1956.

23. Lennox, D. H. and Kelber, C. N. Summary report of the hazards of the Argonaut reactor. U. S. Atomic Energy Commission Report ANL 5647 [Argonne National Laboratory, Lemont, Illinois]. 1959.

24. Murray, Raymond L. Nuclear reactor physics. Englewood Cliffs, N. J. Prentice Hall, Inc. 1957.

25. Olson, R. G. Dynamic simulation of a fast reactor. Nucleonics 15, No. 5: 76-79. May, 1957.

26. O'Meara, F. E. Reactor simulators. Journal of Applied Physics. 24: 1200-1202. 1953.

27. Pagels, Walter. A portable electronic pile kinetic simulator. Transactions of the American Institute of Electrical Engineers. 70: 1422-1426. 1951.

28. Savant, C. J., Jr. Basic feedback control system design. New York, N. Y. McGraw-Hill Book Co., Inc. 1958.

29. Schultz, M. A. Control of nuclear reactors and power plants. New York, N. Y. McGraw-Hill Book Co., Inc. 1955.

ACKNOWLEDGMENTS

The author wishes to express his gratitude to his major professor Dr. Robert E. Uhrig whose guidance and encouragement made this work possible.

Thanks also are due to Dr. Glenn Murphy, head of the Theoretical and Applied Mechanics and Chairman of the Nuclear Engineering Administrative Committee for making available the analog computers and other equipment used in this investigation.

APPENDIX A

Solution of the Time Dependent Reactor Equations

The method used for solving Equations 23, 24, 25 and 26 for the relationships between δK_1 and δK_2 and the stable reactor period are discussed here. For purposes of solution it was assumed that the relationship between the dependent variables (N_1, N_2, C_1 and C_2) and time were of the form

$$N_1 = N_{10} e^{t/\tau} \tag{46}$$

$$N_2 = N_{20} e^{t/\tau} \tag{47}$$

$$C_1 = C_{10} e^{t/\tau} \tag{48}$$

$$C_2 = C_{20} e^{t/\tau} \tag{49}$$

where

N_1, N_2, C_1 and C_2 = neutron and precursor concentrations at time t

N_{10}, N_{20}, C_{10} and C_{20} = neutron and precursor concentrations at time t

τ = reactor period

t = time.

The reactor exhibits a single stable period therefore the periods in Equations 46, 47, 48 and 49 are equal. Substitution of Equations 46, 47, 48 and 49 into Equations 23, 24, 25 and 26 yields the following relationships between N_1 and N_2.

$$\left[7.40 \times 10^3(\delta K)_1 - \frac{1}{\tau} - 48.1 + \frac{48.0(0.0803)}{0.0800 + \frac{1}{\tau}}\right] N_1 \qquad (50)$$

$$+ 7.40 \times 10^3 \alpha N_2 = 0$$

$$\left[7.40 \times 10^3(\delta K)_2 - \frac{1}{\tau} - 48.1 + \frac{48.0(0.0803)}{0.0800 + \frac{1}{\tau}}\right] N_2 \qquad (51)$$

$$+ 7.40 \times 10^3 \alpha N_1 = 0$$

If N_1 and N_2 are not to have trivial solutions, the determinant formed by the coefficients of N_1 and N_2 must equal zero. This results in

$$AD - BC = 0 \qquad (52)$$

where

$$A = 7.40 \times 10^3(\delta K)_1 - \frac{1}{\tau} - 48.1 + \frac{48.0(0.0803)}{0.0800 + \frac{1}{\tau}}$$

$$B = 7.40 \times 10^3 \alpha$$

$$C = 7.40 \times 10^3 \alpha$$

$$D = 7.40 \times 10^3(\delta K)_2 - \frac{1}{\tau} - 48.1 + \frac{(48.0)(0.0803)}{0.0800 + \frac{1}{\tau}} .$$

For the just critical condition Equations 50 and 51 can be solved for δK_1 and δK_2 for various ratios of N_1 to N_2

$$\delta K_1 = -\alpha \frac{N_2}{N_1} \qquad (53)$$

$$\delta K_2 = -\alpha \frac{N_1}{N_2} . \qquad (54)$$

Equations 53 and 54 were used to obtain the reactivity values for each region for the ramp input study and for plotting the critical contour lines of Figures 27 and 29. Equation 52 was used to plot the constant period contour lines of these

figures and Equations 50 and 51 were used to establish the constant neutron density lines.

APPENDIX B

Development of the Reactor Transfer Functions for the Two Core System

The reactor transfer functions for the two core reactor system are derived for a sinusoidal variation of the coupling.

The equations to be solved are

$$\frac{dn_1}{dt} = \frac{\delta K_1 n_1}{\ell} - \frac{\beta n_1}{\ell} + \lambda C_1 + \frac{\alpha n_2}{\ell} \tag{55}$$

$$\frac{dC_1}{dt} = \frac{\beta n_1}{\ell} - \lambda C_1 \tag{56}$$

$$\frac{dn_2}{dt} = \frac{\delta K_2}{\ell} n_2 - \frac{\beta n_2}{\ell} + \lambda C_2 + \frac{\alpha}{\ell} n_1 \tag{57}$$

$$\frac{dC_2}{dt} = \frac{\beta n_2}{\ell} - \lambda C_2 . \tag{58}$$

The symbols in these equations have been defined previously in the text of the thesis. With the introduction of α as a function of time Equations 55 and 57 no longer have constant coefficients, a necessary condition for developing a transfer function. If small excursions of n_1, n_2 and α are assumed these equations can be approximated by a set with constant coefficients. It was therefore assumed that

$$n_1 = n_{10} + \delta n_1 \tag{59}$$

$$n_2 = n_{20} + \delta n_2 \tag{60}$$

$$\alpha = \alpha_o + \delta\alpha \tag{61}$$

$$C_1 = C_{10} + \delta C_1 \tag{62}$$

$$C_2 = C_{20} + \delta C_2 \, . \tag{63}$$

The symbols with the zero subscripts represent the steady state values and the delta terms represent the small excursions. Substitution of Equations 56 and 58 into Equations 55 and 57 results in

$$\frac{dn_1}{dt} = \frac{\delta K_1 n_1}{\ell} - \frac{dC_1}{dt} + \frac{\alpha n_2}{\ell} \tag{64}$$

$$\frac{dn_2}{dt} = \frac{\delta K_2 n_2}{\ell} - \frac{dC_2}{dt} + \frac{\alpha n_1}{\ell} \, . \tag{65}$$

By making the replacement that

$$\frac{dn}{dt} = \frac{dn_o}{dt} + \frac{d\delta n}{dt} = 0 + \frac{d\delta n}{dt} \tag{66}$$

and substituting Equations 59, 60 and 61 into Equations 64 and 65 yields

$$\frac{d\delta n_1}{dt} = \frac{\delta K_1 n_{10}}{\ell} + \frac{\delta K_1 \delta n_1}{\ell} - \frac{d\delta C_1}{dt} + \frac{\alpha_o n_{20}}{\ell} + \frac{\alpha_o \delta n_2}{\ell} + \frac{\delta \alpha n_{20}}{\ell} \tag{67}$$

$$\frac{d\delta n_2}{dt} = \frac{\delta K_2 n_{20}}{\ell} + \frac{\delta K_2 \delta n_2}{\ell} - \frac{d\delta C_2}{dt} + \frac{\alpha_o n_{10}}{\ell} + \frac{\alpha_o \delta n_1}{\ell} + \frac{\delta \alpha n_{10}}{\ell} \, . \tag{68}$$

where terms containing products of delta terms were dropped. When the oscillator is in the mean position the reactor is

just critical and therefore

$$\frac{\delta K_1 n_{10}}{\ell} + \frac{\alpha_o n_{20}}{\ell} = 0 \tag{69}$$

$$\frac{\delta K_2 n_{20}}{\ell} + \frac{\alpha_o n_{10}}{\ell} = 0 . \tag{70}$$

Taking the Laplace transforms of Equations 56, 58, 67 and 68 substituting

$$\frac{d\delta C_1}{dt} = \frac{\beta \delta n_1}{\ell} - \lambda \delta C_1 \tag{71}$$

$$\frac{d\delta C_2}{dt} = \frac{\beta \delta n_2}{\ell} - \lambda \delta C_2 \tag{72}$$

results in

$$\delta n_1(S)\left[S - \frac{\delta K_1}{\ell} + \frac{\beta S}{\ell(s+\lambda)}\right] - \frac{\delta n_2(S)}{\ell}\alpha_o = \frac{n_{20}}{\ell}\delta\alpha(S) \tag{73}$$

$$-\frac{\delta n_1(S)}{\ell}\alpha_o + \delta n_2(S)\left[S - \frac{\delta K_2}{\ell} + \frac{\beta S}{\ell(S+\lambda)}\right] = \frac{n_{10}}{\ell}\delta\alpha(S) . \tag{74}$$

Division of Equation 73 by $d\alpha(S)n_{10}$ and Equation 74 by $d\alpha(S)n_{20}$ results in

$$\frac{\delta n_1(S)}{n_{10}\delta\alpha(S)}\left[S + \frac{\alpha_o}{\ell R} + \frac{\beta S}{\ell(S+\lambda)}\right] - \frac{\delta n_2(S)}{n_{20}\delta\alpha(S)}\frac{\alpha_o}{R\ell} = \frac{1}{R\ell} \tag{75}$$

$$-\frac{\delta n_1(S)}{n_{10}\delta\alpha(S)}R\frac{\alpha_o}{\ell} + \frac{\delta n_2(S)}{n_{20}\delta\alpha(S)}\left[S + \frac{\alpha_o R}{\ell} + \frac{\beta S}{\ell(S+\lambda)}\right] = \frac{R}{\ell} . \tag{76}$$

where R was substituted for N_{10}/N_{20} and $\delta K_1/\ell$ and $\delta K_2/\ell$ were replaced by $-\alpha_o/R$ and $-\alpha_o R$ respectively.

Equations 75 and 76 contain the two transfer functions

$\frac{\delta n_1(s)}{n_{10}\delta\alpha(s)}$ and $\frac{\delta n_2(s)}{n_{20}\delta\alpha(s)}$ which can be obtained by means of determinants, as

$$\frac{\delta n_1(s)}{n_{10}\delta\alpha(s)} = \frac{\begin{vmatrix} \frac{1}{R\ell} & -\frac{\alpha_o}{R\ell} \\ \frac{R}{\ell} & \left[s + \frac{\alpha_o R}{\ell} + \frac{\beta s}{\ell(s+\lambda)}\right] \end{vmatrix}}{\begin{vmatrix} \left[s + \frac{\alpha_o}{\ell R} + \frac{\beta s}{\ell(s+\lambda)}\right] & -\frac{\alpha_o}{R\ell} \\ -\frac{R\alpha_o}{\ell} & \left[s + \frac{\alpha_o R}{\ell} + \frac{\beta s}{\ell(s+\lambda)}\right] \end{vmatrix}} \qquad (77)$$

$$\frac{\delta n_2(s)}{n_{20}\delta\alpha(s)} = \frac{\begin{vmatrix} \left[s + \frac{\alpha_o}{\ell R} + \frac{\beta s}{\ell(s+\lambda)}\right] & \frac{1}{R\ell} \\ -\frac{R\alpha_o}{\ell} & \frac{R}{\ell} \end{vmatrix}}{\begin{vmatrix} \left[s + \frac{\alpha_o}{\ell R} + \frac{\beta s}{\ell(s+\lambda)}\right] & -\frac{\alpha_o}{R\ell} \\ -\frac{R\alpha_o}{\ell} & \left[s + \frac{\alpha_o R}{\ell} + \frac{\beta s}{\ell(s+\lambda)}\right] \end{vmatrix}}. \qquad (78)$$

Equations 77 and 78 are the transfer functions for the two core reactor system. With no flux tilting (R = 1) the two equations are identical, with flux tilting the two equations are different.

APPENDIX C

Component Values and Potentiometer Settings

Table 6. Step inputs of reactivity

Component	Value	Potentiometer	Setting
a	1.000 Megohms	2 A	0.485
b	0.100 Megohms	12 A	variable
c	1.000 Megohms	10 A	0.484
d	0.100 Megohms	2 B	0.373
e	0.999 Megohms	4 A	1.00
f	0.999 Megohms	-	-
g	0.100 Megohms	6 A	1.00
h	0.100 Megohms	-	-
i	10.06 Megohms	8 A	0.810
j	10.05 Megohms	8 B	0.808
k	1.000 Megohms	3 A	0.485
l	0.100 Megohms	13 B	variable
m	1.000 Megohms	11 B	0.482
n	0.100 Megohms	3 B	0.373
o	1.000 Megohms	5 B	1.00
p	1.000 Megohms	-	-
q	0.253 Megohms	7 B	1.000
r	0.253 Megohms	-	-
s	10.07 Megohms	9 A	0.804
t	10.04 Megohms	9 B	0.801

Table 6. (Continued)

Component	Value	Potentiometer	Setting
u	0.01007 Microfarads	-	-
v	1.0036 Microfarads	-	-
w	0.01005 Microfarads	-	-
x	0.9969 Microfarads	-	-

Table 7. Sinusoidal variations of coupling

Component	Value	Potentiometer	Setting
a	0.500 Megohms	11 B	0.502
b	0.500 Megohms	1 A	0.502

Table 8. Ramp inputs of reactivity

Component	Value	Potentiometer	Setting
a	0.500 Megohms	15 A	0.502